

## Reviewer 1

Xie et al. identified and quantified individual nitrogen-containing aromatic compounds (NACs) found in cookstove aerosol produced from water boiling tests. The study focused on two different fuels, charcoal and red oak, and mainly compared and contrasted emissions of NACs from cold start and hot start phases of the WBT. A unique aspect of this study is a focus on filter artifacts by comparing NACs on a quartz fiber filter placed downline of a PTFE membrane. In addition, they quantified the absorption of individual NACs at 365 nm based on their measured concentrations. The authors identified 17 different structures of NACs from their MS-MS spectra. The main conclusions of this study are that the backup quartz fiber filter concentrations of NACs were very high, sometimes even larger than on the front PTFE filter highlighting the importance of understanding these sampling artifacts for quantification of semivolatile species better. They also conclude that the NACs in this study make up less than 5% of the extractable absorption at 365 nm on the PTFE filter.

General comments: The results of this paper should be published because this study quantifies particulate emissions of NACs from cookstoves, which is understudied. The results also demonstrate the need to understand sampling artifacts from filters when they are used for quantitative analysis. However, some of the key conclusions of the paper may be misleading for the reader. For example, it is concluded that <5% of the extractable absorption is from NACs and they not significant brown carbon chromophores in cookstove smoke. However, much higher percentages were observed on the back up quartz filter, some of which may be in the particle phase in the atmosphere.

### **Reply:**

Thanks for the reviewer's comments, and we'll reply these point by point in the reviewer's specific comments.

Here we just want to clarify that NACs were analyzed only for quartz filter samples (front and backup filters,  $Q_f$  and  $Q_b$ ). PTFE filters were commonly used for gravimetric analysis, but were rarely extracted using organic solvents. The installation of a backup quartz filter ( $Q_b$ ) behind a PTFE filter in parallel to a bare quartz filter ( $Q_f$ ) was typically used to estimate the adsorption of gaseous OC ("positive artifact") on the main (or "bare") quartz filter (Subramanian et al., 2004; Watson et al., 2009). This Q-QBT approach presumes that the upstream PTFE filter adsorb no organic gases, and then  $Q_b$  is exposed to organic vapor with the same concentration as  $Q_f$ . It has been shown to provide a robust estimate of the positive artifact on  $Q_f$  OC (McDow and Huntzicker, 1990; Turpin et al., 1994).

In section 2.2 (lines 166-167), we have mentioned that the  $Q_f$  and  $Q_b$  sample extraction and subsequent analysis for NACs were conducted as described in Xie et al. (2019).

To avoid the confusion, the original expressions

*"to evaluate the potential for sampling artifacts of NACs in  $PM_{2.5}$ ."* (lines 120-121)

*"Adsorption artifact was evaluated using a quartz-fiber back-up filter ( $Q_b$ ) installed downstream of the PTFE filter during  $PM_{2.5}$  sampling."* (lines 143-144) have been changed into

*“to evaluate the potential for sampling artifacts of PM<sub>2.5</sub> NACs on the bare quartz filter in parallel.”* (lines 119-120)

*“The adsorption artifact of  $Q_f$  was evaluated using a quartz-fiber back-up filter ( $Q_b$ ) installed downstream of the PTFE filter during PM<sub>2.5</sub> sampling.”* (lines 147-148)

**Specific comments:**

**1.** There are some well-documented problems with WBTs, mostly arguing that their combustion efficiencies don't match those in the real world (Johnson et al., 2008, 2010). If the combustion efficiency in real homes is lower, this could result in less NACs due to less flaming and lower NO<sub>x</sub>. Given this, it would be helpful to have a measure of combustion efficiency, such as modified combustion efficiency, so that it can be compared with field measurements in the future. This may be possible, given the paper mentions gaseous pollutants were measured (Line 140). Even without this, it would be helpful to have more of a description of the cookstoves and WBTs which would help with the interpretation of the results.

**Reply:**

As mentioned in the manuscript (page 5, lines 116-118; page 7, lines 151-152), the OC and EC emissions, as well as the absorption of methanol extractable OC from cookstove combustions were reported in our previous work (Xie et al., 2018). In that study, the measurement data of modified combustion efficiency (MCE), overall thermal efficiency (OTE) and emission factors (EFs) of OC and EC for each fuel-cookstove combination were provided in supplementary information.

To make the results of this study comparable to field measurements in the future, we added MCE data for each fuel-cookstove combination in Table S1.

*“Tables S1 and S2 summarized the measurement results of  $Q_f$  and  $Q_b$ , respectively, for each fuel-cookstove combination, including concentrations of carbon contents and light-absorbing properties of sample extracts. As the light absorption of BB BrC is expected to depend largely on burn conditions (Saleh et al., 2014; Pokhrel et al., 2016), the MCE and EC/OC ratio, two indicators of burn conditions, are also given in Table S1.”* (lines 160-165)

The descriptions of the cookstoves and WBT protocol were added when replying to comments 1a and 1b.

**1a.** The stoves are listed in tables in the supplement; however, they are not really discussed in the experimental section of the main paper. How are they different? Where are they used around the world?

**Reply:**

In our previous study (Xie et al., 2018), the light absorption of organic carbon emitted from burning red oak wood and charcoal in cookstoves were investigated using the same samples as this work. That study also provided modified combustion efficiency (MCE) data, overall thermal efficiency (OTE), and emission factors (EFs) of OC and EC for each fuel-cookstove combination during high power phases of the water boiling test, showing the difference across fuel-specific cookstoves.

In the revised manuscript, we added a brief description of each fuel-specific cookstove in supplementary information (Text S1).

*“A brief description of each fuel-specific cookstove was given in supplementary information (Text S1)” (Lines 141–142)*

**1b.** Please include more information about the water boiling tests in the experimental section, as most readers of the journal will not be familiar with it. You should also mention the simmer phase is included for the hot start sample in some tests, if this is correct.

**Reply:**

In the revised manuscript, we added more information on the three test phases in the experimental section.

*“Both CS and HS phases are defined by the duration between the ignition and the water boils. The CS phase starts with the cookstove, pot, and water at ambient temperature; the HS immediately follows the CS with the cookstove hot but the pot and water at ambient temperature; and the SIM phase is defined by a 30-min time period with the cookstove hot and water temperature maintained at 3 °C below the boiling point.” (lines 134-139)*

The emission test of each fuel-cookstove combination contained a simmer (SIM) phase. Except the 3-stone fire, emission factors (EFs) of OC and EC at the SIM phase were substantially lower than those at high power phases (CS and HS) (Xie et al., 2018). Then, BrC absorption and its molecular composition were primarily measured for CS- and HS-phase samples. In the current work, the SIM-phase samples were analyzed only for red oak burning in a 3-stone fire. This test had comparable OC emissions between CS- and SIM-phase combustions (Xie et al., 2018), and the CS and HS phases of the 3-stone fire are typically similar and cannot be separated. The three SIM-phase samples from the 3-stone fire were treated as HS-phase samples of other cookstove tests. These information on sample selection were originally provided in supplementary information of the manuscript. To make it clear, we moved the information on sample selection to the experiment section of the main text.

*“Details for determinations of OCEC concentrations and BrC absorption were provided in supplementary information (Text S2). Except the 3-stone fire, EFs of OC and EC at the SIM phase were substantially lower than those at high power phases (CS and HS), so the BrC absorption from red oak and charcoal burning were primarily measured for CS- and HS-phase samples in Xie et al. (2018). The SIM-phase samples were analyzed only for red oak burning in a 3-stone fire. This test had comparable OC emissions between CS- and SIM-phase combustions, and CS and HS phases of the 3-stone fire were typically similar and could not be separated (Xie et al., 2018). In the current work, the same emission samples were selected for the analysis of NACs, and the three SIM-phase samples from the 3-stone fire were treated as HS-phase samples of other cookstove tests.” (Lines 151-160)*

**1c.** Could use more reasoning as to how red oak and charcoal are different as seen in Figure S1 C and F by relating hot start and cold start phases to the observed types of combustion. For example, hot start is mostly smoldering for charcoal (high OC emissions with very low BC and therefore low NO<sub>x</sub> to make less NACs).

**Reply:**

Thanks for the reviewer’s suggestions.

In Table S1, the MCE values of charcoal burning indicate that the HS-phase burning is more smoldering than the CS-phase burning. However, the mass ratio of total NACs to OC in percentages ( $tNAC_{OC}\%$ ) showed no significant difference ( $p = 0.29$ ) between HS and CS phases. Considering that the EC/OC ratio of charcoal burning was more sensitive to the initial temperature in the cookstove than MCE variations, it could not be used to predict burn conditions, BrC absorption, or NACs formation from charcoal burning.

Figure S1c and f are used to illustrate the dependence of NACs formation on burn conditions for red oak and charcoal combustions, respectively. Unlike biomass burning, the EC/OC ratio might not be used to parameterize burn conditions of charcoal in cookstoves. We provided a preliminary explanation on the difference of  $tNAC_{OC}\%$  between red oak and charcoal combustions in lines 221-224.

*“Wood burning generates more volatile aromatic compounds (e.g., phenols, PAHs) than charcoal burning (Kim Oanh, et al., 1999), and NACs can form when aromatic compounds and reactive nitrogen (e.g.,  $NO_x$ ) are present during solid fuel combustion (Lin et al., 2016, 2017).”*

In comparison to red oak burning, charcoal combustion was more smoldering with significant smaller MCE values ( $p < 0.01$ ). The wood fire tends to have reduced emissions of  $NO_x$  from the smoldering phase (Bertschi et al., 2003). But charcoal and wood are different fuels, and the emission factors (EFs) of  $NO_x$  were not measured for controlled cookstove tests in this work. Bhattacharya et al. (2002) reported the EFs of  $NO_x$  from a number of traditional and improved cookstoves. They found that EFs for  $NO_x$  using wood was slightly lower than charcoal. Then we might not infer that the charcoal burning should emit less  $NO_x$  to form NACs in this work.

In the revised manuscript, the original expression

*“Like  $MAC_{365}$  and  $\dot{A}_{abs}$  in  $Q_f$  samples for charcoal burning (Xie et al., 2018),  $tNAC_{OC}\%$  derived from the same samples did not correlate with EC/OC ratios in this work (Fig. S1f). Xie et al. (2018) found that the HS-phase for charcoal burning had average OC EFs 5–10 times higher than the CS-phase, while the EC EFs decreased by more than 90% from the CS- to HS-phase, so the EC/OC for charcoal burning is sensitive to the initial temperature in the cookstove, and cannot be used to predict burn conditions, BrC absorption, or NACs formation.”* (lines 253-258)

has been changed into

*“In Table S1, the MCE values of charcoal burning indicate that the HS-phase is more smoldering than the CS-phase. However, the average  $tNAC_{OC}\%$  values showed no significant difference ( $p = 0.29$ ) between HS and CS phases. Like  $MAC_{365}$  and  $\dot{A}_{abs}$  in  $Q_f$  samples for charcoal burning (Xie et al., 2018),  $tNAC_{OC}\%$  derived from the same samples did not correlate with EC/OC ratios in this work (Fig. S1f). Xie et al. (2018) found that the HS-phase for charcoal burning had average OC EFs 5–10 times higher than the CS-phase, while the EC EFs decreased by more than 90% from the CS- to HS-phase. Furthermore, no correlation has been observed between MCE and EC/OC for charcoal burning at the HS-phase. So, the EC/OC for charcoal burning tends to depend more on the initial temperature in the cookstove than MCE variations, and cannot be used to predict burn conditions, BrC absorption, or NACs formation.”* (lines 276-285)

2. Regarding source apportionment for NAC measurements (Lines 385-402), these fractions of NAC/OM will be very different in the field because OM can come from many sources. The NAC should be ratioed to a combustion product such as CO or EC.

**Reply:**

In the original manuscript, Figure 2 presents mass fraction patterns of individual NACs in OM from cookstove combustions using red oak wood and charcoal, open biomass burning, and photochemical reactions of typical aromatic precursors with NO<sub>x</sub>. Receptor models are commonly used for source apportionment of particulate pollutants in the atmosphere (Jaeckels et al., 2007; Shrivastava et al., 2007; Xie et al., 2013), and assume that the ambient pollutants measured in the field are linear combinations from a number of time-variant sources/factors. When using field measurement data of NACs for receptor modeling, the resulting factors can be linked with specific emission sources by comparing with the NAC patterns shown in Figure 2 of this work. Further studies are warranted to unveil NACs patterns of other potential sources (e.g., motor vehicle emissions).

As we mentioned in the introduction, besides combustion sources, atmospheric NACs can also be generated through secondary pathways (lines 106-107). EC is specifically related to primary combustion sources, and CO is totally in the gas phase. In the current work, the gas-phase concentrations of NACs were not available.

To clarify the application of NAC patterns in source apportionment, we added some statement in lines 419-420 and 434-437.

*“This difference among NACs may help with source apportionment using receptor models, which are commonly used and assume that the ambient pollutants measured in the field are linear combinations from a number of time-variant sources/factors. (Jaeckels et al., 2007; Shrivastava et al., 2007; Xie et al., 2013).”*

*“When using field measurement data of NACs for receptor modeling, the resulting factors can be linked with specific emission sources by comparing with the NAC patterns shown in Fig. 2. Further studies are also warranted to unveil NAC patterns of other potential sources (e.g., motor vehicle emissions).”*

**3.** It is implied in lines 412-420 that NACs identified in this study are not significant BrC chromophores, however, if the quartz filter (Qb) is included the fraction is likely higher. It may be more appropriate to give an upper limit given that NACs on Qb could partition into the particle phase in the atmosphere. It is difficult to conclude that NACs are not significant BrC chromophores given the measurements on the sampling artifact that other studies have not considered. Also, NACs may be higher for fuel/stove/cooking activity combinations that result in more flaming combustion which produces NO<sub>x</sub>, an important reactant for NAC formation. Another factor is that the fractional absorption by NACs was not directly measured. Surrogates were used to quantify NAC concentrations and approximate MACs were used to calculate the Abs<sub>365</sub>.

**Reply:**

In the manuscript, we mentioned that most identified NACs are strong BrC chromophores, as the average contributions of total NACs to Abs<sub>365</sub> of sample extracts were more than one order of magnitude higher than their average mass contributions.

*“The average contributions of total NACs to Abs<sub>365</sub> (Abs<sub>365,tNAC%</sub>) of the sample extracts (Q<sub>f</sub> 1.10 – 2.57%, Q<sub>b</sub> 10.7 – 21.0%) are up to 10 times greater than their average tNAC<sub>OC%</sub> (Q<sub>f</sub> 0.31 – 1.01%, Q<sub>b</sub> 1.08 – 3.31%, Table 1). Considering that some NACs are not light-absorbing (Table S4) and the OM/OC ratio is typically greater than*

unity, most NACs that contribute to Abs<sub>365</sub> are strong BrC chromophores.” (Lines 446-450)

Due to the lack of authentic standards, the quantification of NACs concentrations and their contributions to Abs<sub>365</sub> of Q<sub>f</sub> extracts are subject to uncertainties. However, there are evidences showing that BrC absorption is majorly contributed by large molecules with MW > 500 – 1000 Da (Di Lorenzo and Young, 2016; Di Lorenzo et al., 2017). Large NACs molecules may be generated from cookstoves with flaming combustions, and their structures and light absorption are worth future investigations. In previous studies on ambient and biomass burning particles, most identified NACs had a MW lower than 300 – 500 Da, and their total contributions to bulk BrC absorption were estimated to be less than 10% (Mohr et al., 2013; Zhang et al., 2013; Teich et al., 2017; Xie et al., 2019). Similar results were also obtained in the current work. Even if the identified NACs on Q<sub>b</sub> are totally derived from evaporation of the upstream filter (negative artifact), the adjusted average contributions of total NACs (Q<sub>f</sub> + Q<sub>b</sub>) to Abs<sub>365</sub> of Q<sub>f</sub> extracts are still lower than 5% (1.59 – 4.01%). Therefore, we suggest that further studies are needed to identify large BrC molecules (including high MW NACs) in ambient and source particles.

The original text from lines 412 to 420 has been changed into

*“All identified NACs explained 1.10 – 2.58% (Fig. S3) of Q<sub>f</sub> extracts absorption. Even if the NACs on Q<sub>b</sub> were totally derived from upstream filter evaporation, the adjusted average contributions of total NACs (Q<sub>f</sub> + Q<sub>b</sub>) to Abs<sub>365</sub> of Q<sub>f</sub> extracts were still lower than 5% (1.59 – 4.01%). Due to the lack of authentic standards, the quantification of NACs concentrations and their contributions to Abs<sub>365</sub> of Q<sub>f</sub> extracts might be subject to uncertainties. However, growing evidences showed that BrC absorption was majorly contributed by large molecules with MW > 500 – 1000 Da (Di Lorenzo and Young, 2016; Di Lorenzo et al., 2017). Large molecules of NACs may be generated from flaming combustions in cookstoves, and their structures and light absorption are worth future investigations. In previous studies on ambient and biomass burning particles, most identified NACs had a MW lower than 300 – 500 Da, and their total contributions to bulk BrC absorption were estimated to be less than 10% (Mohr et al., 2013; Zhang et al., 2013; Teich et al., 2017; Xie et al., 2019). Similar results were also obtained in the current work. Therefore, further studies are needed to identify large BrC molecules (including high MW NACs) in ambient and source particles.”* (Lines 457-471)

**4.** It is assumed that because Abs<sub>365,tNAC%</sub> at 365 nm is 7-11 times higher on the quartz fiber backup filter, that NACs may be important light absorbers in the gas phase (lines 442, 425-429, 432-434). To claim this in the paper, more discussion and reasoning for should be given.

**4a.** Those on the backing filter are not necessarily in the gas phase in the natural environment. As you explain in the paper, there are both positive and negative artifacts and there is not likely a straightforward way of calculating what would be in the gas phase.

**Reply:**

Thanks for the reviewer’s suggestions. As we mentioned in the original manuscript, the NACs on Q<sub>b</sub> were contributed by both positive (gaseous adsorption) and negative (filter evaporation) sampling artifacts. However, the relative contributions



of positive and negative artifacts to  $Q_b$  measurements are unknown. Furthermore, gas-phase NACs were not collected using an upstream denuder or an adsorbent cartridge downstream of the filter, and future work is needed to understand the gas/particle distribution of NACs in the ambient and source emissions. Due to the lack of gas-phase NACs data, we overstated that gaseous NACs might be an important group of light-absorbing species in the atmosphere.

The conclusions on light absorption of gaseous NACs has been deleted. Section 3.4 has been reorganized as follows.

*“The average  $Abs_{365,iNAC}\%$  values of  $Q_f$  and  $Q_b$  samples are presented by fuel type and WBT phase in the Fig. 3 stack plots, and experimental data for each fuel-cookstove are provided in Tables S11–S14. The average contributions of total NACs to  $Abs_{365}$  ( $Abs_{365,iNAC}\%$ ) of the sample extracts ( $Q_f$  1.10 – 2.57%,  $Q_b$  10.7 – 21.0%) are up to 10 times greater than their average  $tNAC_{OC}\%$  ( $Q_f$  0.31 – 1.01%,  $Q_b$  1.08 – 3.31%, Table 1). Considering that some NACs are not light-absorbing (Table S4) and the OM/OC ratio is typically greater than unity, most NACs that contribute to  $Abs_{365}$  are strong BrC chromophores. Like the mass composition of NACs (Fig. 1),  $C_{10}H_7NO_3$  (CS 0.24%, HS 0.43%) and  $C_8H_9NO_5$  (CS 1.22%, HS 0.55%) were the major contributors to  $Abs_{365}$  for the  $Q_f$  samples collected during red oak and charcoal burning, respectively (Fig.3a). The average  $Abs_{365,iNAC}\%$  of  $Q_b$  samples are 7.53 to 11.3 times higher than those of  $Q_f$  samples. Unlike the  $Q_f$  samples from red oak burning,  $C_{10}H_{11}NO_5$  (CS 2.77%, HS 3.09%) has the highest average contribution to  $Abs_{365}$  for  $Q_b$  samples, followed by  $C_{10}H_7NO_3$  (CS 1.96%, HS 1.32%) and  $C_8H_9NO_5$  (CS 1.32%, HS 1.44%). While  $C_8H_9NO_5$  dominated the contribution (CS 8.78%, HS 5.82%) to  $Abs_{365}$  for the  $Q_b$  samples from charcoal burning (Fig. 3b). All identified NACs explained 1.10 – 2.58% (Fig. S3) of  $Q_f$  extracts absorption. Even if the NACs on  $Q_b$  were totally derived from upstream filter evaporation, the adjusted average contributions of total NACs ( $Q_f + Q_b$ ) to  $Abs_{365}$  of  $Q_f$  extracts were still lower than 5% (1.59 – 4.01%). Due to the lack of authentic standards, the quantification of NACs concentrations and their contributions to  $Abs_{365}$  of  $Q_f$  extracts might be subject to uncertainties. However, growing evidences showed that BrC absorption was majorly contributed by large molecules with MW > 500 – 1000 Da (Di Lorenzo and Young, 2016; Di Lorenzo et al., 2017). Large molecules of NACs may be generated from flaming combustions in cookstoves, and their structures and light absorption are worth future investigations. In previous studies on ambient and biomass burning particles, most identified NACs had a MW lower than 300 – 500 Da, and their total contributions to bulk BrC absorption were estimated to be less than 10% (Mohr et al., 2013; Zhang et al., 2013; Teich et al., 2017; Xie et al., 2019). Similar results were also obtained in the current work. Therefore, further studies are needed to identify large BrC molecules (including high MW NACs) in ambient and source particles.”* (Lines 444-471)

**4b.** The vapor pressures of these molecules are very low, and the fraction in the gas phase is low. However, for some nitroaromatics such as 2-nitrophenol the vapor pressure is higher. Are the concentrations for some molecules higher on the back up filter compared to the front filter and do we expect them to have higher vapor pressures?

**Reply:**

Due to the lack of measurement data of gas-phase NACs, the gas-phase fractions of NACs are unknown. 4-Nitrophenol (not 2-nitrophenol) was identified and quantified using authentic standards in this work. As the vapor pressure of NACs were rarely

measured or estimated in literatures, the Toxicity Estimation Software Tool (T.E.S.T) developed by the United States Environmental Protection Agency (US EPA) was used to predict subcooled vapor pressure of selected NACs standards at 25 °C ( $p^{o,*}_L$ ) in the following Table.

Standard compounds	Formula	$m/z$ , [M-H] <sup>-</sup>	Vapor pressure (atm)
4-Nitrophenol	C <sub>6</sub> H <sub>5</sub> NO <sub>3</sub>	138.0196	1.58 × 10 <sup>-5</sup>
2-Methyl-4-nitrophenol	C <sub>7</sub> H <sub>7</sub> NO <sub>3</sub>	152.0353	4.57 × 10 <sup>-6</sup>
4-Nitrocatechol	C <sub>6</sub> H <sub>5</sub> NO <sub>4</sub>	154.0145	3.37 × 10 <sup>-7</sup>
2-Methyl-5-nitrobenzoic acid	C <sub>8</sub> H <sub>7</sub> NO <sub>4</sub>	180.0302	1.07 × 10 <sup>-8</sup>
2-Nitro-1-naphthol	C <sub>10</sub> H <sub>7</sub> NO <sub>3</sub>	188.0353	4.62 × 10 <sup>-8</sup>

In comparison to the vapor pressure of *n*-alkanes and polycyclic aromatic hydrocarbons (PAHs) predicted by Xie et al. (2103, 2014), NACs listed in the above table are mostly more volatile than henicane and fluoranthene (~10<sup>-8</sup> atm). Xie et al. (2014) found that the gas-phase concentrations of *n*-alkanes and PAHs with vapor pressure greater than henicane and fluoranthene were comparable or higher than their particle-phase concentrations. Furthermore, the average  $Q_b$  to  $Q_f$  mass ratios of the 17 individual NACs ranged from 54.3 ± 24.5% to 135 ± 52.4%, comparable to *n*-alkanes with carbon number ≤ 21 (e.g., henicane; 26.3 – 163%) and PAHs with benzene ring number ≤ 4 (e.g., fluoranthene; 46.3 – 134%) in the ambient (Xie et al., 2014). So, we suspect that the identified NACs in this study may have substantial fractions remaining in the gas-phase.

In the revised manuscript, more discussions on NACs volatility were added in the last paragraph of section 3.2.

*“In this work, the average  $Q_b$  to  $Q_f$  mass ratios of the 17 individual NACs ranged from 50.8 ± 13.4% to 140 ± 52.9%, comparable to *n*-alkanes with carbon number ≤ 21 (e.g., henicane; 26.3 – 163%) and PAHs with benzene ring number ≤ 4 (e.g., fluoranthene; 46.3 – 134%) in the ambient of urban Denver (Xie et al., 2014). Xie et al. (2014) found that the gas-phase concentrations of *n*-alkanes and PAHs with vapor pressure greater than henicane and fluoranthene were comparable or higher than their particle-phase concentrations. The vapor pressure of five NACs standards at 25 °C ( $p^{o,*}_L$ ) were predicted using the US EPA Toxicity Estimation Software Tool (T.E.S.T) and listed in Table S10. Their  $p^{o,*}_L$  values are mostly higher than henicane and fluoranthene (~10<sup>-8</sup> atm; Xie et al., 2013, 2014). Then the identified NACs in this study may have substantial fractions remaining in the gas phase.”* Lines (332-341)

**4c.** What are the absorption cross sections for these molecules in the gas phase and their expected gaseous concentrations that would lead us to believe they are significant? Are they long-lived enough in the gas phase to be important? Only solution phase MACs at 365 nm are used to claim that gas phase absorption is significant and this is not sufficient.

**Reply:**

Thanks for the reviewer’s comments.

In the current work, NACs from cookstove emissions were identified and quantified using filter samples only. The gas-phase concentrations, absorption cross sections, and life times of identified NACs were not measured or predicted. So, we



overstated that gaseous NACs might be an important group of light-absorbing species in the atmosphere. The conclusions on light absorption of gaseous NACs has been deleted.

5. Line 132: Omit that you did kerosene tests. It is not critical as you do not discuss these results.

**Reply:**

The expression in the method section has been changed as suggested. We omitted kerosene tests.

## References

- Bertschi, I., Yokelson, R. J., Ward, D. E., Babbitt, R. E., Susott, R. A., Goode, J. G., and Hao, W. M.: Trace gas and particle emissions from fires in large diameter and belowground biomass fuels, *Journal of Geophysical Research: Atmospheres*, 108, 10.1029/2002JD002100, 2003.
- Bhattacharya, S. C., Albina, D. O., and Abdul Salam, P.: Emission factors of wood and charcoal-fired cookstoves, *Biomass and Bioenergy*, 23, 453-469, [https://doi.org/10.1016/S0961-9534\(02\)00072-7](https://doi.org/10.1016/S0961-9534(02)00072-7), 2002.
- Di Lorenzo, R. A., and Young, C. J.: Size separation method for absorption characterization in brown carbon: Application to an aged biomass burning sample, *Geophysical Research Letters*, 43, 458-465, 10.1002/2015gl066954, 2016.
- Di Lorenzo, R. A., Washenfelder, R. A., Attwood, A. R., Guo, H., Xu, L., Ng, N. L., Weber, R. J., Baumann, K., Edgerton, E., and Young, C. J.: Molecular-Size-Separated Brown Carbon Absorption for Biomass-Burning Aerosol at Multiple Field Sites, *Environmental Science & Technology*, 51, 3128-3137, 10.1021/acs.est.6b06160, 2017.
- Jaekels, J. M., Bae, M. S., and Schauer, J. J.: Positive matrix factorization (PMF) analysis of molecular marker measurements to quantify the sources of organic aerosols, *Environmental Science & Technology*, 41, 5763-5769, 10.1021/es062536b, 2007.
- McDow, S. R., and Huntzicker, J. J.: Vapor adsorption artifact in the sampling of organic aerosol: Face velocity effects, *Atmospheric Environment. Part A. General Topics*, 24, 2563-2571, [https://doi.org/10.1016/0960-1686\(90\)90134-9](https://doi.org/10.1016/0960-1686(90)90134-9), 1990.
- Mohr, C., Lopez-Hilfiker, F. D., Zotter, P., Prévôt, A. S. H., Xu, L., Ng, N. L., Herndon, S. C., Williams, L. R., Franklin, J. P., Zahniser, M. S., Worsnop, D. R., Knighton, W. B., Aiken, A. C., Gorkowski, K. J., Dubey, M. K., Allan, J. D., and Thornton, J. A.: Contribution of Nitrated Phenols to Wood Burning Brown Carbon Light Absorption in Detling, United Kingdom during Winter Time, *Environmental Science & Technology*, 47, 6316-6324, 10.1021/es400683v, 2013.
- Shrivastava, M. K., Subramanian, R., Rogge, W. F., and Robinson, A. L.: Sources of organic aerosol: Positive matrix factorization of molecular marker data and comparison of results from different source apportionment models, *Atmospheric Environment*, 41, 9353-9369, 10.1016/j.atmosenv.2007.09.016, 2007.
- Subramanian, R., Khlystov, A. Y., Cabada, J. C., and Robinson, A. L.: Positive and Negative Artifacts in Particulate Organic Carbon Measurements with Denuded and Undenuded Sampler Configurations Special Issue of Aerosol Science and Technology on Findings from the Fine Particulate Matter Supersites Program, *Aerosol Science and Technology*, 38, 27-48, 10.1080/02786820390229354, 2004.
- Teich, M., van Pinxteren, D., Wang, M., Kecorius, S., Wang, Z., Müller, T., Močnik, G., and Herrmann, H.: Contributions of nitrated aromatic compounds to the light absorption of water-soluble and particulate brown carbon in different atmospheric environments in Germany and China, *Atmospheric Chemistry and Physics*, 17, 1653-1672, 10.5194/acp-17-1653-2017, 2017.
- Turpin, B. J., Huntzicker, J. J., and Hering, S. V.: Investigation of organic aerosol sampling artifacts in the los angeles basin, *Atmospheric Environment*, 28, 3061-3071, [https://doi.org/10.1016/1352-2310\(94\)00133-6](https://doi.org/10.1016/1352-2310(94)00133-6), 1994.
- Watson, J. G., Chow, J. C., Chen, L. W. A., and Frank, N. H.: Methods to Assess Carbonaceous Aerosol Sampling Artifacts for IMPROVE and Other Long-Term Networks, *Journal of the Air & Waste*

- Management Association, 59, 898-911, 10.3155/1047-3289.59.8.898, 2009.
- Xie, M., Piedrahita, R., Dutton, S. J., Milford, J. B., Hemann, J. G., Peel, J. L., Miller, S. L., Kim, S.-Y., Vedal, S., Sheppard, L., and Hannigan, M. P.: Positive matrix factorization of a 32-month series of daily PM<sub>2.5</sub> speciation data with incorporation of temperature stratification, *Atmospheric Environment*, 65, 11-20, <http://dx.doi.org/10.1016/j.atmosenv.2012.09.034>, 2013.
- Xie, M., Shen, G., Holder, A. L., Hays, M. D., and Jetter, J. J.: Light absorption of organic carbon emitted from burning wood, charcoal, and kerosene in household cookstoves, *Environmental Pollution*, 240, 60-67, <https://doi.org/10.1016/j.envpol.2018.04.085>, 2018.
- Xie, M., Chen, X., Hays, M. D., and Holder, A. L.: Composition and light absorption of N-containing aromatic compounds in organic aerosols from laboratory biomass burning, *Atmospheric Chemistry and Physics*, 19, 2899-2915, 10.5194/acp-19-2899-2019, 2019.
- Zhang, X., Lin, Y.-H., Surratt, J. D., and Weber, R. J.: Sources, Composition and Absorption Ångström Exponent of Light-absorbing Organic Components in Aerosol Extracts from the Los Angeles Basin, *Environmental Science & Technology*, 47, 3685-3693, 10.1021/es305047b, 2013.

## Reviewer 2

This manuscript presents the analysis of N-containing aromatic compounds (NAC) in PM<sub>2.5</sub> samples collected from biomass-burning emissions of wood and charcoal in special household stoves. Prior to the HPLC analysis, the collected filters were spiked with one deuterated internal standard and extracted in methanol. The goal of this research was to estimate the contribution of BrC NAC species to the total absorption of PM<sub>2.5</sub> samples. The authors also discussed the differences (in OC, total NAC, individual NACs, etc.) between the hot-start and cold-start phases, and also between front and back filters. The authors acknowledged the limitations of this study (e.g., no gas-phase NACs were measured). This study is scientifically important, since NACs are not only light-absorbing compounds, but also are toxic organic species and they are still not well characterized. The manuscript is well organized and well written. I have a few major comments. In summary, I recommend this manuscript for publication after major revisions

### **Reply:**

Thanks for the reviewer's comments, and we'll reply these point by point in the reviewer's specific comments.

### **Major comments:**

1. The filter samples were spiked with only one deuterated I.S. compound (4-nitrophenol-d<sub>4</sub>, C6), while the analyzed NACs (Fig 1) have different volatility levels (C7-C11). The author should check if there were potential losses of I.S., which is more volatile than the rest of the analyzed species, and if these losses led to a large overestimates of the concentrations of the analyzed compounds.

### **Reply:**

In this study, the NACs in filter samples were determined identically as Xie et al. (2017, 2019). To minimize the evaporation loss, the sample extract volume was reduced using rotary evaporator under a vacuum, but not nitrogen blowdown evaporation. The coefficient of variation (CV) of the peak area for internal standard (IS) was only 0.16, indicating a stable IS signal. In addition, method recoveries were determined by spiking blank filters with known amounts of standard compounds, followed by extraction and quantification in the same way as that for collected samples. At the end of section 2.2, we mentioned that the average recoveries of NAC standards on pre-baked blank filters ranged from 75.1% to 116% (Lines 197-198). Therefore, the measurement results were not subject to uncertainties due to the loss of internal standard.

2. The manuscript contains a lot of abbreviations, which made it very hard to read (HS, CS, Qf, Qb, WBT, OMMs, SIM, etc.)

### **Reply:**

We have defined each abbreviation in the abstract and the rest of the text at the first instance, which satisfied the requirement of the journal.

3. Table 1. The concentrations of the total NACs are strikingly high for the backup filters. I am wondering if some sort of unexpected breakthrough happened during the

sampling (especially in the case of charcoal burning). Would it be possible that the BB emissions were quite hot during the sampling, which caused the evaporation from the front filter?

**Reply:**

The mass concentrations of OC and EC were measured for the same filter samples in our previous work (Xie et al., 2018). As no EC has been detected on backup filters ( $Q_b$ ), the breakthrough of particles was not expected during the sampling.

As shown in Table S2, filter samples were mostly collected at ambient temperature (~25 °C). We suspect that the identified NACs in this work have substantial fractions remaining in the gas phase (Lines 332-341).

In lines 344-347, we mentioned that the filter samples were mostly collected near ambient temperature.

*“Considering that most of the  $Q_f$  and  $Q_b$  samples were collected near ambient temperature (Table S2, ~25 °C), the composition of NACs derived from  $Q_f$  measurements alone can be biased due to the lack of gas-phase measurements.”*

4. Some minor comments Line 130. U.S. EPA – please make sure abbreviations are explained in the text Line 131: “USA” should be added after “NC” Line 126, what is “Jiko Poa”? Should company name be added? Lines 152, 156 etc. Company name (+city, state, country) of material and instruments is missing.

**Reply:**

In the revised manuscript, we defined US EPA before it first appeared (Lines 128-129).

“USA” was added after “NC” in line 130.

We added a brief description for all cookstoves, including “Jiko Poa”, in supplementary information (Text S1). The company and country names (BURN Manufacturing, Kenya) were added right after “Jiko Poa” (Line 141).

Company, state, and country were added for materials and instruments in lines 169-170, 173.

## References

- Xie, M., Chen, X., Hays, M. D., Lewandowski, M., Offenberg, J., Kleindienst, T. E., and Holder, A. L.: Light Absorption of Secondary Organic Aerosol: Composition and Contribution of Nitroaromatic Compounds, *Environmental Science & Technology*, 51, 11607-11616, 10.1021/acs.est.7b03263, 2017.
- Xie, M., Shen, G., Holder, A. L., Hays, M. D., and Jetter, J. J.: Light absorption of organic carbon emitted from burning wood, charcoal, and kerosene in household cookstoves, *Environmental Pollution*, 240, 60-67, <https://doi.org/10.1016/j.envpol.2018.04.085>, 2018.
- Xie, M., Chen, X., Hays, M. D., and Holder, A. L.: Composition and light absorption of N-containing aromatic compounds in organic aerosols from laboratory biomass burning, *Atmospheric Chemistry and Physics*, 19, 2899-2915, 10.5194/acp-19-2899-2019, 2019.

### Reviewer 3

This manuscript is a nice piece of work describing the emission of nitrogen containing aromatic compounds (NAC) from the use of cookstoves. The authors aim to understand the contribution of these species to the light absorption of organic matter in PM<sub>2.5</sub> at the wavelength of 365 nm. The authors found that much higher contribution of NAC light absorption to PM<sub>2.5</sub> in quartz fiber backup filters than in PTFE front filters, suggesting that NAC may be an important group of light absorbing compounds in the gas phase. In addition, the authors found the NAC compounds targeted in this manuscript ( $M_w < 300$ ) are less important for the light absorption of PM<sub>2.5</sub> bound organic matter at least from cookstove emissions, and indicate that larger molecules with  $M_w > 500$  are responsible for the light absorption of organic matters. The manuscript is well written, and I recommend publication of this manuscript after addressing minor technical corrections outlined below.

#### **Reply:**

Thanks for the reviewer's comments, and we'll reply these point by point in the reviewer's specific comments.

#### **Specific comments:**

1. If it is possible, the authors should present all NAC in emission factors ( $\text{g kg}^{-1}$ ) rather than in mass concentrations ( $\mu\text{g m}^{-3}$ ). Emission factors are more useful than mass concentrations as they can be used for emission control strategies directly.

#### **Reply:**

In this work, the target is to characterize the composition, structures, and light absorption of NACs from cookstove emissions. The results will improve our understanding on BrC chromophores and sources. To exhibit NACs composition and absorption, their mass concentrations in filter samples should be provided.

As we mentioned in the manuscript, the emissions of OC and EC for the same cookstove tests were reported in our previous work (Xie et al., 2018) (lines 150-151). The emission factors (EFs) of total NACs ( $\text{g kg}^{-1}$  dry fuel) can be obtained from the EFs of OC and the mass ratios of total NACs to OC. In the revised manuscript, the EFs of total NACs were given in Table S5.

**Table S5. Average emission factors of total NACs and OC**

Fuel & Test phase	Red Oak		Charcoal	
	CS	HS <sup>a</sup>	CS	HS
	<b>Front filter (<math>Q_f</math>)</b>			
Sample number	18	17 <sup>b</sup>	15	15
total NAC ( $\text{mg kg}^{-1}$ dry fuel)	$1.18 \pm 0.58$	$1.23 \pm 0.69$	$0.79 \pm 0.65$	$1.40 \pm 0.65$
OC ( $\text{mg kg}^{-1}$ dry fuel)	$244 \pm 170$	$340 \pm 326$	$179 \pm 114$	$619 \pm 368$
	<b>Backup filter (<math>Q_b</math>)</b>			
Sample number	18	17 <sup>b</sup>	14 <sup>b</sup>	15
total NAC ( $\text{mg kg}^{-1}$ dry fuel)	$0.55 \pm 0.24$	$0.61 \pm 0.38$	$0.62 \pm 0.53$	$1.83 \pm 0.79$
OC ( $\text{mg kg}^{-1}$ dry fuel)	$30.5 \pm 17.6$	$38.2 \pm 24.8$	$66.5 \pm 38.9$	$196 \pm 96.2$

<sup>a</sup> Including three SIM phase samples from the 3-stone fire; <sup>b</sup> one filter sample was missed for analysis.



“The EFs of total NACs shown in Table S5 were obtained by multiplying the EFs of OC and tNACoc%.” (Lines 218-219)

2. Line 171: ng \_L should be ng/μL or ng μL<sup>-1</sup>.

**Reply:**

Revised as suggested. (Line 188)

3. Line 214 onwards: This assumes that the backup quartz fiber filter can trap all the gas phase compounds and does not have a breakthrough at all. A better way to estimate the artifact of a filter sampling system is to utilize a denuder in front of a PTFE filter for gas sampling and place a quartz fiber filter after the PTFE to correct a negative artifact from blown-off. It would be good if the authors discuss briefly here about the potential usage of the denuder for the artifact correction in addition to the backup quartz fiber filter.

**Reply:**

Thanks for the reviewer’s suggestions.

The backup quartz filter was typically used to evaluate the adsorption of gaseous organics (“positive artifact”) on filter media. This method does not assume that the backup filter can trap all the gas-phase compounds. We mentioned that the gas-phase NACs were not measured in this study (lines 344-347), and concluded “*Further studies are warranted to investigate the gas/particle distribution of NACs in the ambient and source emissions.*” (Lines 481-482)

In the revised manuscript, we added a few descriptions on the use of a denuder to avoid positive artifacts and its potential issues.

“*A denuder upstream of the filter for gas sampling was used to avoid positive artifact in several studies (Ding et al., 2002; Ahrens et al., 2012). This approach can generate large negative artifacts by altering the gas-particle equilibrium after the denuder, and a denuder efficiency of 100% might not be guaranteed (Kirchstetter et al., 2001; Subramanian et al., 2004).*” (Lines 238-242)

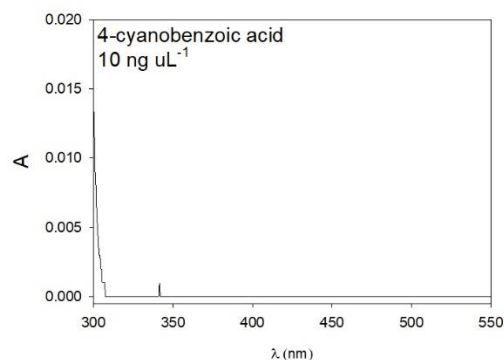
4. Line 283: In Table S3, the authors suggest C<sub>8</sub>H<sub>5</sub>NO<sub>2</sub> as 3-cyanobenzoic acid. This is commercially available from several chemical suppliers, and it can be positively identified if C<sub>8</sub>H<sub>5</sub>NO<sub>2</sub> correspond to the authors’ suggestion. I ask the authors to purchase the standard compound and quantify it instead of using a surrogate compound.

**Reply:**

Thanks for the reviewer’s suggestion.

After testing the three isomers of cyanobenzoic acid (2-, 3-, and 4-cyanobenzoic acid), the C<sub>8</sub>H<sub>5</sub>NO<sub>2</sub> molecule from cookstove emissions was identified as 4-cyanobenzoic acid. So, the mass concentration and absorption of C<sub>8</sub>H<sub>5</sub>NO<sub>2</sub> were quantified using 4-cyanobenzoic acid.

We have updated the tables and figures with C<sub>8</sub>H<sub>5</sub>NO<sub>2</sub> throughout the manuscript. As shown in the figure below, 4-cyanobenzoic acid has no light absorption at > 350 nm. Thus, the contribution of C<sub>8</sub>H<sub>5</sub>NO<sub>2</sub> to Abs<sub>365</sub> of sample extracts is 0.



5. Fig S5: The mass spectrometric conditions and ionization methods used to obtain MS2 spectra for some compounds shown in Fig S5 are very different from ones shown in Fig S4, and they are not comparable at all. I ask the authors to remove those (EI and ESI+) from Fig S5 as they cannot be compared to each other.

**Reply:**

The MS-MS spectra of  $C_8H_7NO_4$  and  $C_9H_9NO_4$  showed the loss of OCN (Fig. S4g, m), suggesting a structure of benzoxazole/benzisoxazole or the presence of cyanate ( $-O-C\equiv N$ ) or isocyanate ( $-O=C=N$ ) groups. To identify the structure of the OCN group, the MS and MS-MS spectra of four standard compounds, including phenyl cyanate ( $C_6H_5OCN$ ), benzoxazole ( $C_7H_5NO$ ), 4-methoxyphenyl isocyanate ( $CH_3OC_6H_4NCO$ ), and 2,4-dimethoxyphenyl isocyanate [ $(CH_3O)_2C_6H_3NCO$ ] were obtained from Xie et al. (2019) and shown in Fig. S5 (i-n). These compounds do not have a phenol structure and cannot be detected using ESI under negative ion mode. Fig. S5 (i-n) suggest that the loss of an OCN group only happens during the fragmentation of phenyl cyanate. If Fig. S5 (i-n) is removed, we cannot identify the phenyl cyanate feature for  $C_8H_7NO_4$  and  $C_9H_9NO_4$  (Lines 380-386).

*“The MS-MS spectra of  $C_8H_7NO_4$  eluting at 8.14 min (Fig. S3e) and  $C_9H_9NO_4$  eluting at 9.22 min (Fig. S3j) indicate the loss of OCN (Fig. S4g, m), suggesting benzoxazole/benzisoxazole structure or the presence of cyanate ( $-O-C\equiv N$ ) or isocyanate ( $-O=C=N$ ) groups. Mass spectra of selected standard compounds (Fig. S5i-n) in our previous work (Xie et al. 2019) show the loss of an OCN group only happens during the fragmentation of phenyl cyanate. Thus, the  $C_8H_7NO_4$  and  $C_9H_9NO_4$  isomers containing OCN indicate a phenyl cyanate feature.”*

Xie et al. (2019) identified the phenyl cyanate structure for NACs from open biomass burning in a same way. Therefore, we kept these mass spectra in supplementary information.

**References**

- Xie, M., Shen, G., Holder, A. L., Hays, M. D., and Jetter, J. J.: Light absorption of organic carbon emitted from burning wood, charcoal, and kerosene in household cookstoves, *Environmental Pollution*, 240, 60-67, <https://doi.org/10.1016/j.envpol.2018.04.085>, 2018.
- Xie, M., Chen, X., Hays, M. D., and Holder, A. L.: Composition and light absorption of N-containing aromatic compounds in organic aerosols from laboratory biomass burning, *Atmospheric Chemistry and Physics*, 19, 2899-2915, [10.5194/acp-19-2899-2019](https://doi.org/10.5194/acp-19-2899-2019), 2019.

1 Chemical composition, structures, and light absorption of N-containing  
2 aromatic compounds emitted from burning wood and charcoal in  
3 household cookstoves

带格式的: 段落间距段后: 0 磅

4  
5 Mingjie Xie<sup>1</sup>, Zhenzhen Zhao<sup>1</sup>, Amara L. Holder<sup>2</sup>, Michael D. Hays<sup>2</sup>, Xi Chen<sup>2</sup>, Guofeng Shen<sup>3</sup>,  
6 [Wyatt M. Champion<sup>2</sup>](#), James J. ~~Jetter<sup>2</sup>~~[Jetter<sup>2</sup>](#), Qin'geng ~~Wang<sup>4</sup>~~[Wang<sup>4</sup>](#)

7  
8 <sup>1</sup>Collaborative Innovation Center of Atmospheric Environment and Equipment Technology,  
9 Jiangsu Key Laboratory of Atmospheric Environment Monitoring and Pollution Control, School  
10 of Environmental Science and Engineering, Nanjing University of Information Science &  
11 Technology, 219 Ningliu Road, Nanjing 210044, China

12 ~~<sup>2</sup>Center for Environmental Measurement and Modeling~~, Office of Research and Development, U.S.  
13 Environmental Protection Agency, 109 T.W. Alexander Drive, Research Triangle Park, NC 27711,  
14 USA

15 <sup>3</sup>Laboratory for Earth Surface Processes, College of Urban and Environmental Sciences, Peking  
16 University, Beijing 100871, China

17 <sup>4</sup>State Key Laboratory of Pollution Control and Resource Reuse, Nanjing University, Nanjing  
18 210023, China

19  
20 *Correspondence to:* Mingjie Xie

21 *Email:* ~~(~~[mingjie.xie@colorado.edu](mailto:mingjie.xie@colorado.edu); [mingjie.xie@nuist.edu.cn](mailto:mingjie.xie@nuist.edu.cn)~~)~~

22 Tel: +1-18851903788;

23 Fax: +86-25-58731051;

24 Mailing address: 219 Ningliu Road, Nanjing, Jiangsu, 210044, China

25

26

27 **Abstract**

28 N-containing aromatic compounds (NACs) are an important group of light-absorbing  
29 molecules in the atmosphere. They are often observed in combustion emissions, but their chemical  
30 formulas and structural characteristics remain uncertain. In this study, red oak wood and charcoal  
31 fuels were burned in cookstoves using the standard water boiling test (WBT) procedure.  
32 Submicron aerosol particles in the cookstove emissions were collected using quartz ( $Q_f$ ) and  
33 polytetrafluoroethylene (PTFE) filter membranes positioned in parallel. A back-up quartz filter  
34 ( $Q_b$ ) was also installed downstream of the PTFE filter to evaluate the effect of sampling artifact on  
35 NACs measurements. Liquid chromatography-mass spectroscopy (LC-MS) techniques identified  
36 seventeen NAC chemical formulas in the cookstove emissions. The average concentrations of total  
37 NACs in  $Q_b$  samples ( $0.37 \pm 0.31 - 1.789 \pm 0.787 \mu\text{g m}^{-3}$ ) were greater than 50% of those observed  
38 in the  $Q_f$  samples ( $0.4751 \pm 0.403 - 3.5491 \pm 1.632.06 \mu\text{g m}^{-3}$ ), and the  $Q_b$  to  $Q_f$  mass ratios of  
39 individual NACs had a range of 0.02 – 2.71, indicating that the identified NACs might have  
40 substantial fractions remaining in the gas-phase. In comparison to other sources, cookstove  
41 emissions from red oak or charcoal fuels did not exhibit unique NAC structural features, but had  
42 distinct NACs composition. However, before identifying NACs sources by combining their  
43 structural and compositional information, the gas-particle partitioning behaviors of NACs should  
44 be further investigated. The average contributions of total NACs to the light absorption of organic  
45 matter at  $\lambda = 365 \text{ nm}$  ( $1.10 - 2.587\%$ ) in  $Q_f$  ~~samples are much lower than those in~~ and  $Q_b$  samples  
46 ( $10.7 - 21.0\%$ ) are up to 10 times larger than their mass contributions ( $Q_f$  0.31 – 1.01%,  $Q_b$  1.08 –  
47 3.31%), so the identified NACs are mostly strong light absorbers. To explain more sample extracts  
48 absorption, These results suggest that more research/future research is needed to understand the  
49 chemical and optical properties of ~~gaseous chromophores and heavier~~ high molecular weight (e.g.,  
50 MW > 500 Da) entities in particulate matter.

51

## 52 **1 Introduction**

53 In the developing world, 2.8 billion people burn solid fuels in household cookstoves for  
54 domestic activities such as heating and cooking (Bonjour et al., 2013). A variety of gaseous and  
55 ~~particulate-particle~~-phase pollutants — carbon monoxide (CO), nitrogen oxides (NO<sub>x</sub>), volatile  
56 organic compounds (VOCs), fine particulate matter with aerodynamic diameter  $\leq 2.5 \mu\text{m}$  (PM<sub>2.5</sub>),  
57 black carbon (BC), organic carbon (OC), etc. — are emitted from cookstoves largely due to  
58 incomplete combustion (Jetter et al., 2012; Shen et al., 2012; Wathore et al., 2017). In China, the  
59 relative contributions of residential coal and biomass burning (BB) to annual PM<sub>2.5</sub> emissions  
60 decreased from 47% (4.32 Tg) in 1990 to 34% (4.39 Tg) in 2005 due to the growth in industrial  
61 emissions (Lei et al., 2011). Although, more than half of BC (> 50 %) and OC (> 60 %) emissions  
62 are attributed to residential coal and BB in both China and India (Cao et al., 2006; Klimont et al.,  
63 2009; Lei et al., 2011).

64 Household solid fuel combustion is a leading human health risk, especially for women and  
65 children who tend to spend more time indoors than men (Anenberg et al., 2013). Estimates show  
66 that exposures to PM<sub>2.5</sub> from domestic solid fuel combustion caused 3.9 million premature deaths  
67 and ~4.8% of lost healthy life years (Smith et al., 2014). In addition, the emissions of carbonaceous  
68 aerosols from cookstoves can affect the Earth's radiative balance by absorbing and scattering  
69 incoming solar radiation (Lacey and Henze, 2015; Aunan et al., 2009). BC is the most efficient  
70 light absorber in the atmosphere, while the total aerosol absorption, including that from OC, is still  
71 highly uncertain (Yang et al., 2009; Park et al., 2010; Feng et al., 2013; Wang et al., 2014; Tuccella  
72 et al., 2020). Multiple field and laboratory studies have demonstrated that OC in both primary PM  
73 emissions (e.g., biomass and fossil fuel combustions) and secondary organic aerosol (SOA) feature



74 a range of absorptivity in the near ultraviolet (UV) and short visible wavelength regions  
75 (Nakayama et al., 2010; Forrister et al., 2015; Lin et al., 2015; De Haan et al., 2017; Xie et al.,  
76 2017a, b, 2018). The light absorbing OC fraction is often referred to as “brown carbon” (BrC).  
77 Unlike open BB (e.g., forest, grassland, and cropland fires) — one of the most important primary  
78 sources for organic aerosols (Bond et al., 2004) — the light absorption of BrC from household  
79 cookstove emissions is rarely investigated. Sun et al. (2017) found that the BrC absorption from  
80 residential coal burning accounted for 26.5% of the total aerosol absorption at 350–850 nm. BrC  
81 from wood combustion in cookstoves has a greater mass specific absorption than that from open  
82 BB over the wavelength range of 300 – 550 nm (Xie et al., 2018). These results suggest that  
83 cookstove emissions may also be an important BrC source, which needs to be accounted for  
84 separately from open BB.

85 Organic molecular markers (OMMs) are commonly used in receptor-based source  
86 apportionment of carbonaceous aerosols (Jaekels et al., 2007; Shrivastava et al., 2007; Xie et al.,  
87 2012). Polycyclic aromatic hydrocarbons (PAHs) and their derivatives are a group of OMMs with  
88 light absorption properties dependent on ring number or the degree of conjugation (Samburova et  
89 al., 2016). As discussed in Xie et al. (2019), PAHs are generated from a multitude of combustion  
90 processes (e.g., BB, fossil fuel combustion) (Chen et al., 2005; Riddle et al., 2007; Samburova et  
91 al., 2016), and their ubiquitous nature makes them less than ideal OMMs for BrC source attribution.  
92 Because of the specific toxicological concern raised by PAHs — they are mutagenic and  
93 carcinogenic [International Agency for Research on Cancer (IARC), 2010] — source emission  
94 factors (EFs), ambient levels, and potential health effects of PAHs are investigated exhaustively  
95 (Ravindra et al., 2008; Kim et al., 2013). Similar to PAHs, N-containing aromatic compounds  
96 (NACs) are a group of BrC chromophores commonly detected in ambient PM and source

97 emissions. Zhang et al. (2013) and Teich et al. (2017) calculated the absorption of individual NACs  
98 in aqueous extracts of ambient PM, the total of which explained ~3% of the bulk extract absorption  
99 at 365 – 370 nm. With the same approach, Xie et al. (2017a, 2019) found that the absorbance due  
100 to NACs in BB or secondary OC was 3 – 10 times higher than their mass contributions. Lin et al.  
101 (2016, 2017) estimated an absorbance contribution of 50 – 80% from NACs in BB OC directly  
102 from their high-performance liquid chromatography (HPLC)/photodiode array (PDA) signals,  
103 which are subject to considerable uncertainty due to the co-elution of other BrC chromophores  
104 (e.g., PAHs and their derivatives). These results indicate that NACs are strong BrC chromophores,  
105 but the estimation of their contributions to BrC absorption depends largely on how well they are  
106 chemically characterized. Nitrophenols, methyl nitrophenols, nitrocatechols and methyl  
107 nitrocatechols (including isomers) are typical atmospheric NACs (Claeys et al., 2012; Desyaterik  
108 et al., 2013; Zhang et al., 2013). These NACs can be generated from BB (Lin et al., 2016, 2017;  
109 Xie et al., 2019), fossil fuel combustion (Lu et al., 2019), and the reactions of aromatic volatile  
110 organic compounds (VOCs) with reactive nitrogen species (e.g., NO<sub>x</sub>) (Xie et al., 2017a), and are  
111 not unique to specific sources (e.g., BB). By using a HPLC interfaced to a diode array detector  
112 (DAD) and quadrupole (Q) time-of-flight mass spectrometer (ToF-MS), Xie et al. (2019) found  
113 that BB NACs contain methoxy and cyanate groups. Nitronaphthol, nitrobenzenetriol, and methyl  
114 nitrobenzenetriol are characteristic NACs for NO<sub>x</sub>-based chamber reactions of naphthalene,  
115 benzene, and *m*-cresol, respectively (Xie et al., 2017a). Yet, few studies have investigated the  
116 composition of NACs from household cookstove emissions (Fleming et al., 2018; Lu et al., 2019).

117       The present study aims to characterize NACs in PM<sub>2.5</sub> from burning red oak and charcoal in  
118 a variety of cookstoves and calculate their contributions to bulk OC absorption. The absorption of  
119 OC in solvent extracts of cookstove emissions were measured in our previous work (Xie et al.,

120 2018). Presently, NACs are identified and quantified using an earlier described HPLC/DAD-Q-  
121 ToF-MS system. In addition, the NACs adsorbed on a backup quartz filter downstream of a  
122 polytetrafluoroethylene (PTFE) membrane filter are analyzed, to evaluate the potential for  
123 sampling artifacts of PM<sub>2.5</sub> NACs in PM<sub>2.5</sub> on the bare quartz filter in parallel. This work unveils  
124 BrC composition at a molecular level and increases the understanding of BrC chromophores and  
125 their sources. It also shows that further identification of large molecules (e.g., > 500 Da) may better  
126 explain BrC absorption in the particle phase ~~and that understanding the light absorption of gaseous~~  
127 ~~chromophores is important for the future.~~

## 128 **2 Methods**

### 129 **2.1. Cookstove emissions sampling**

130 ~~Details of t~~The cookstove emission test facility, fuel-cookstove combinations, water boiling  
131 test (WBT) protocol, and PM<sub>2.5</sub> emissions sampling were described previously in Jetter and  
132 Kariher (2009) and Jetter et al. (2012) and Xie et al. (2018). Briefly, the cookstove emissions tests  
133 were performed at the United States Environmental Protection Agency (U.S. EPA) cookstove test  
134 facility in Research Triangle Park, NC, USA. ~~Three fuels (Red oak wood, and lump charcoal,~~  
135 ~~and 1-K kerosene)~~ were burned in fuel-specific cookstoves under controlled conditions. Emissions  
136 tests for each fuel-cookstove combination were performed in triplicate. The WBT protocol  
137 (version 4) (Global Alliance for Clean Cookstoves, 2014) is designed to measure cookstove power,  
138 energy efficiency, and fuel use, and contains cold-start (CS) high power, hot-start (HS) high power,  
139 and simmer (SIM) low power phases. Both CS and HS phases are defined by the duration between  
140 the ignition and the water boils. The CS phase starts with the cookstove, pot, and water at ambient  
141 temperature; the HS immediately follows the CS with the cookstove hot but the pot and water at  
142 ambient temperature; and the SIM phase is defined by a 30-min time period with the cookstove

143 ~~hot and water temperature maintained at 3 °C below the boiling point. Due to the limited sample~~  
144 ~~number ( $n = 6$ ) and low OC emissions from kerosene burning, only red oak and charcoal burning~~  
145 ~~samples were used for NACs analysis.~~ Low moisture (~10%) oak and charcoal fuels were burned  
146 with five specific-designed cookstove types (Tables S1 and S2); high moisture (~30%) oak fuels  
147 were burned in one cookstove (Jiko Poa, [BURN Manufacturing, Kenya](#)). ~~A brief description of~~  
148 ~~each fuel-specific cookstove was given in supplementary information (Text S1). Emissions tests~~  
149 ~~for each fuel-cookstove combination were performed in triplicate. The WBT protocol (version 4)~~  
150 ~~(Global Alliance for Clean Cookstoves, 2014) is designed to measure cookstove power, energy~~  
151 ~~efficiency and fuel use and utilizes cold start (CS) high power, hot start (HS) high power, and~~  
152 ~~simmer (SIM) low power phases.~~ Gaseous pollutant (e.g., CO, methane (CH<sub>4</sub>)) emissions were  
153 monitored continuously, and PM<sub>2.5</sub> filter samples were collected during each test phase of the WBT  
154 protocol. ~~The modified combustion efficiency (MCE), defined as  $CO_2/(CO_2 + CO)$  on a molar~~  
155 ~~basis, was calculated and discussed in Xie et al. (2018).~~ A quartz-fiber filter (Q<sub>f</sub>) and a PTFE  
156 membrane filter positioned in parallel collected PM<sub>2.5</sub> isokinetically at a flow rate of 16.7 L min<sup>-1</sup>.  
157 ~~The Adsorption artifact of Q<sub>f</sub> was evaluated using a quartz-fiber back-up filter (Q<sub>b</sub>) installed~~  
158 ~~downstream of the PTFE filter during PM<sub>2.5</sub> sampling.~~

## 159 2.2. Chemical analysis

160 The OC and elemental carbon (EC) emissions and UV-Vis light absorption properties (BrC)  
161 of methanol-extracted cookstove particles were reported in Xie et al. (2018). ~~Details of for the~~  
162 ~~method determinations of OCEC concentrations and BrC absorption, sample selection were~~  
163 ~~provided in supplementary information (Text S2). Except the 3-stone fire, EFs of OC and EC at~~  
164 ~~the SIM phase were substantially lower than those at high power phases (CS and HS), so the BrC~~  
165 ~~absorption from red oak and charcoal burning were primarily measured for CS- and HS-phase~~

设置了格式: 字体: 倾斜, 下标

166 samples in Xie et al. (2018). The SIM-phase samples were analyzed only for red oak burning in a  
167 3-stone fire. This test had comparable OC emissions between CS- and SIM-phase combustions,  
168 and CS and HS phases of the 3-stone fire were typically similar and could not be separated (Xie et  
169 al., 2018). In the current work, the same emission samples were selected for the analysis of NACs,  
170 and the three SIM-phase samples from the 3-stone fire were treated as HS-phase samples of other  
171 cookstove tests. Tables S1 and S2 summarized the measurement results of  $Q_f$  and  $Q_b$ , respectively,  
172 for each fuel-cookstove combination, including concentrations of carbon contents and light-  
173 absorbing properties of sample extracts. As the light absorption of BB BrC is expected to depend  
174 largely on burn conditions (Saleh et al., 2014; Pokhrel et al., 2016), the MCE and EC/OC ratio,  
175 two indicators of burn conditions, are also given in Table S1, and measurement results are  
176 summarized in supplementary information (Text S1, Tables S1 and S2).

177 The  $Q_f$  and  $Q_b$  sample extraction and subsequent analysis for NACs were conducted as  
178 described in Xie et al. (2019). In brief, an aliquot of each filter sample was pre-spiked with 250 ng  
179 nitrophenol-d4 (internal standard) and extracted ultrasonically twice for 15 min in 3-5 mL of  
180 methanol. After filtration (30 mm diameter-  $\times 0.2 \mu\text{m}$  pore size, PTFE filter, National Scientific Co.  
181 Ltd, TN, USA), the extract volume was reduced to  $\sim 500 \mu\text{L}$  with rotary evaporation prior to  
182 HPLC/DAD-MS (Q-ToF) analysis. The NACs targeted in this work were chromatographed using  
183 an Agilent 1200 Series HPLC equipped with a Zorbax Eclipse Plus C18 column (2.1 mm  $\times$  100  
184 mm, 1.8  $\mu\text{m}$  particle size; Agilent Technologies, CA, USA). The gradient separation was  
185 performed using water (eluent A) and methanol (eluent B) containing 0.2% acetic acid (v/v) with  
186 a total flow rate of  $0.2 \text{ mL min}^{-1}$ . The eluent B fraction was held at 25% for 3 min, increased to  
187 100% over the next 7 min, where it was held for 22 min, and then returned to 25% over 5 min. An  
188 Agilent 6520 Q-ToF MS equipped with a multimode ion source operating in electrospray



189 ionization (ESI) negative (-) mode was used to determine the chemical formula, molecular weight  
190 (MW), and quantity of each target compound. All sample extracts were analyzed in full scan mode  
191 over 40–1000 Da. A mass accuracy of  $\pm 10$  ppm was selected for compound identification and  
192 quantification. Samples with individual NACs exhibiting the highest MS signal intensities in full  
193 scan mode were re-examined in targeted MS-MS mode using a collision-induced dissociation  
194 (CID) technique. The MS-MS spectra of target NACs  $[M-H]^-$  ions were acquired to deduce  
195 structural information. Similar to bulk carbon and light absorption measurements, NACs were  
196 primarily determined for CS- and HS-phase samples with substantial OC loadings.

197 Due to the limited availability of authentic standards, many of the NACs identified in  
198 cookstove combustion samples were quantified using surrogate compounds with similar MW or  
199 structures. An internal standard method with a 9-point calibration curve ( $\sim 0.01 - 2 \text{ ng } \mu\text{L}^{-1}$ ) was  
200 applied for quantification of concentrations. The compounds represented by each identified NAC  
201 formula were quantified individually and combined to calculate the mass ratio of total NACs to  
202 OC ( $\mu\text{g m}^{-3}$ )  $\times 100\%$  (tNAC<sub>OC</sub>%). Presently, the organic matter (OM) to OC ratio was not  
203 measured or estimated for cookstove combustion emissions, so tNAC<sub>OC</sub>% could be up to 2 times  
204 greater than the contributions of NACs to OM (Reff et al., 2009; Turpin and Lim, 2001). Table S3  
205 lists the chemical formulas, proposed structures, and standard assignments for the NACs identified  
206 here. The quality assurance and control (QA/QC) procedures for filter extraction and instrumental  
207 analysis were the same as Xie et al. (2017a, 2019). NACs were not detected in field blank and  
208 background samples. The average recoveries of NAC standards on pre-spiked blank filters ranged  
209 from 75.1% to 116%, and the method detection limit had a range of 0.70–17.6 pg.

### 210 **2.3. Data analysis**

设置了格式: 上标

211 In Xie et al. (2017a), the DAD measurement directly identified the chemical compounds in  
212 chamber SOA responsible for light absorption in the near UV and visible light ranges. However,  
213 no light absorption from individual NACs was detected in the DAD chromatograms from open BB  
214 (Xie et al., 2019) and cookstove emissions (this work). So the contributions of individual NACs  
215 to light absorption coefficient ( $Abs_{\lambda}$ ,  $Mm^{-1}$ ) for each sample extract at 365 nm ( $Abs_{365,iNAC}\%$ ) were  
216 calculated using the method described in Xie et al. (2017a, 2019):

$$217 \quad Abs_{365,iNAC}\% = \frac{C_{iNAC} \times MAC_{365,iNAC}}{Abs_{365}} \times 100\% \quad (1)$$

218 where  $C_{iNAC}$  is the mass concentration ( $ng\ m^{-3}$ ) of individual NACs, and  $MAC_{365,iNAC}$  is the mass  
219 absorption coefficient ( $MAC_{\lambda}$ ,  $m^2\ g^{-1}$ ) of individual NACs at 365 nm.  $Abs_{365}$  is the light absorption  
220 coefficient ( $Mm^{-1}$ ) of each sample extract at 365 nm, and has been widely used to represent BrC  
221 absorption (Chen and Bond, 2010; Hecobian et al., 2010; Liu et al., 2013). Each NAC compound  
222 was assumed to absorb as a standard (Table S3), of which the  $MAC_{365,iNAC}$  value was obtained  
223 from Xie et al. (2017a, 2019) and listed in Table S4. In this work, Student's  $t$ -test was used to  
224 determine if the means of two sets of data are significantly different from each other, and a  $p$  value  
225 less than 0.05 indicates significant difference.

## 226 **3 Results and discussion**

### 227 **3.1 Summary of total NACs concentration from cookstove emissions**

228 Table 1 summarizes the average concentrations of total NACs and average  $tNAC_{OC}\%$  for  
229  $Q_f$  and  $Q_b$  by fuel type and WBT phase. The EFs of total NACs shown in Table S5 were obtained  
230 by multiplying the EFs of OC and  $tNAC_{OC}\%$ . Filter samples of emissions from burning red oak  
231 wood show-had significantly ( $p < 0.05$ ) higher average total NAC concentrations and  $tNAC_{OC}\%$   
232 than the charcoal burning samples. Wood burning generates more volatile aromatic compounds  
233 (e.g., phenols, PAHs) than charcoal burning (Kim Oanh, et al., 1999), and NACs can form when

234 aromatic compounds and reactive nitrogen (e.g., NO<sub>x</sub>) are present during solid fuel combustion  
235 (Lin et al., 2016, 2017). While burning red oak, emissions from the CS and HS phases show similar  
236 average NAC concentrations, ~~and tNAC<sub>OC</sub>%, and NAC EFs~~ (Tables ~~1 and S5~~). Additionally,  
237 burning low moisture red oak in the Jiko Poa stove had higher tNAC<sub>OC</sub>% than burning high  
238 moisture red oak (Tables S6 and S7), but the difference was not significant ( $p > 0.05$ ). ~~or high~~  
239 ~~moisture red oak in the Jiko Poa stove shows no significant ( $p > 0.05$ ) difference in tNAC<sub>OC</sub>%~~  
240 ~~(Tables S5 and S6).~~ Thus, the NAC ~~and OC~~ emissions from red oak burning are less likely  
241 influenced by WBT phase, and the effect of fuel moisture content needs further investigation ~~or~~  
242 ~~fuel moisture~~. For charcoal fuel samples, compared with the CS-phase, the HS-phase shows  
243 significantly higher ( $p < 0.05$ ) average NAC concentrations. This is likely due to the increase in  
244 OC with the HS phase (Tables 1 and S5 ~~Table 4~~), as the average tNAC<sub>OC</sub>% values are much closer  
245 for the CS- (0.38 ~~40~~ ± 0.25%) and HS-phases (0.31 ± 0.22 ~~21~~%).

246 Several studies have placed a quartz-fiber filter behind a PTFE filter to evaluate the positive  
247 adsorption artifact — adsorption of gas-phase compounds onto particle filter media, “blow-on”  
248 effect (Peters et al., 2000; Subramanian et al., 2004; Watson et al., 2009; Xie et al., 2014). This  
249 method is expected to provide a consistent estimate irrespective of sampling time, but may over  
250 correct the positive artifact by 16–20% due to volatilization of OC off the upstream PTFE filter  
251 (negative artifact, “blow-off” effect) (Subramanian et al., 2004). A denuder upstream of the filter  
252 for gas sampling was used to avoid positive artifact in several studies (Ding et al., 2002; Ahrens  
253 et al., 2012). This approach can generate large negative artifacts by altering the gas-particle  
254 equilibrium after the denuder, and a denuder efficiency of 100% might not be guaranteed  
255 (Kirchstetter et al., 2001; Subramanian et al., 2004). The present study is the first to consider  
256 sampling artifact when measuring semivolatile NACs. This concept merits consideration as

设置了格式: 字体: 倾斜

257 quantification of particle-phase NACs may be subject to large uncertainty. Table 1 shows that the  
258 average concentrations of total NACs on  $Q_b$  ( $0.37 \pm 0.31 - 1.78-79 \pm 0.78-77 \mu\text{g m}^{-3}$ ) are greater  
259 than 5950% and 7980% of those on  $Q_f$  ( $0.47-51 \pm 0.40-43 - 3.54-91 \pm 1.632.06 \mu\text{g m}^{-3}$ ) for red oak  
260 and charcoal burning, respectively. The average  $Q_b$  to  $Q_f$  ratio in percentage using OC  
261 concentrations is 2-3 times lower ( $14.8 \pm 3.87 - 38.8 \pm 18.9\%$ ). Hence, the NACs identified in this  
262 work are present in the relatively volatile bulk OC fraction emitted from cookstoves, and the NACs  
263 in the  $Q_f$  samples may also be present in the gas-phase in the atmosphere. Charcoal burning  
264 emissions show even higher ( $p < 0.05$ )  $Q_b$  to  $Q_f$  total NAC mass ratios (CS 87.784.1  $\pm$  34.238.0%,  
265 HS 143-140  $\pm$  51.452.9%) than red oak burning (CS 53.050.8  $\pm$  40.613.4%, HS 55.13.4  $\pm$   
266 24.726.2%), which is largely due to the higher OC loads on  $Q_f$  ~~samples~~ from red oak burning. Xie  
267 et al. (2018) assumed previously that the  $Q_b$ -adsorbed OC represented the positive sampling  
268 artifact only, and adjusted the light absorbing properties of OC on  $Q_f$  by subtracting  $\text{Abs}_{365}$  and  
269 OC of  $Q_b$  samples directly. In this study, the high  $Q_b$  to  $Q_f$  ratios of total NACs indicate that the  
270 volatilization of NACs from upstream PTFE filter cannot be neglected, but the relative  
271 contributions of positive and negative artifacts to  $Q_b$  measurements are unknown. Therefore, the  
272 measurement results of NACs in  $Q_f$  and  $Q_b$  samples were provided separately, and no correction  
273 was conducted for  $Q_f$  measurements in this work. Since the gaseous NACs adsorbed ~~on~~ in  $Q_b$   
274 samples depends on  $Q_f$  loadings,  $\text{tNACoc}\%$  and total NACs concentrations in each  $Q_f$ - $Q_b$  pair from  
275 matching tests are significantly correlated ( $p < 0.05$ , Fig. S1a, b, d, and e).

276 Along with modified combustion efficiency (MCE), the EC/OC and BC/OA (organic  
277 aerosol) ratios were used previously as indicators of biomass burning conditions (McMeeking et  
278 al., 2014; Pokhrel et al., 2016). Here the burn condition indicates general flame intensity or  
279 combustion temperature (Chen and Bond, 2010; Saleh et al., 2014), and is parameterized to

280 investigate combustion processes (e.g., pyrolysis). The MCE, EC/OC and BC/OA ratios are key  
281 to understanding particulate OC absorptivity (Saleh et al., 2014; Lu et al., 2015) and NACs  
282 formation from open BB (Xie et al., 2019). Presently, the relationships of tNAC<sub>OC</sub>% versus EC/OC  
283 for Q<sub>f</sub> samples are shown in Fig. S1c and f by fuel type. Because no significant difference was  
284 observed for average total NACs concentrations, tNAC<sub>OC</sub>%, and EC/OC ratios when testing CS-  
285 versus HS- phases during red oak fuel burning, the CS- and HS-phases were pooled for a regression  
286 analysis. The tNAC<sub>OC</sub>% of Q<sub>f</sub> samples positively correlate ( $r = 0.83$ ,  $p < 0.05$ ) with EC/OC for red  
287 oak burning (Fig. S1c), as observed in Xie et al. (2019) for open BB, which suggests that burn  
288 conditions influence NACs formation during BB. Note that the NAC concentrations on Q<sub>f</sub> were  
289 possibly adsorbed while in a gaseous state, while EC is particle phase.

290 In Table S1, the MCE values of charcoal burning indicate that the HS-phase is more  
291 smoldering than the CS-phase. However, the average tNAC<sub>OC</sub>% values showed no significant  
292 difference ( $p = 0.29$ ) between HS and CS phases. Like MAC<sub>365</sub> and  $\dot{A}_{abs}$  in Q<sub>f</sub> samples for charcoal  
293 burning (Xie et al., 2018), tNAC<sub>OC</sub>% derived from the same samples did not correlate with EC/OC  
294 ratios in this work (Fig. S1f). Xie et al. (2018) found that the HS-phase for charcoal burning had  
295 average OC EFs 5–10 times higher than the CS-phase, while the EC EFs decreased by more than  
296 90% from the CS- to HS-phase. Furthermore, no correlation has been observed between MCE  
297 and EC/OC for charcoal burning at the HS-phase. ~~So~~ the EC/OC for charcoal burning ~~is~~ tends  
298 to depend ~~more on~~ sensitive to the initial temperature in the cookstove ~~than~~ MCE variations, and  
299 cannot be used to predict burn conditions, BrC absorption, or NACs formation.

### 300 3.2 Composition of NACs in Q<sub>f</sub> and Q<sub>b</sub>

301 During solid fuel combustion, NACs may form from aromatic compounds (e.g., substituted  
302 phenols) and reactive nitrogen species (e.g., NH<sub>3</sub>, NO<sub>x</sub>, and HONO) in both the gas- and particle-

303 phase (Harrison et al., 2005; Kwamena and Abbatt, 2008; Lu et al., 2011; Lin et al., 2016, 2017).  
304 Aromatic hydrocarbons are produced during fuel pyrolysis (Simoneit et al., 1993; Simoneit, 2002;  
305 Kaal et al., 2009). Oxidation of fuel derived nitrogen, rather than molecular nitrogen in air, is the  
306 major formation pathway of reactive nitrogen species (Glarborg et al., 2003).

307 Presently, seventeen chemical formulas were identified as NACs in cookstove emissions,  
308 several of which are widely observed in ambient air and open BB particles (e.g., C<sub>6</sub>H<sub>5</sub>NO<sub>3</sub>,  
309 C<sub>6</sub>H<sub>5</sub>NO<sub>4</sub>) (Claeys et al., 2012; Zhang et al., 2013; Lin et al., 2016, 2017; Xie et al., 2019). Figure  
310 1 shows the average concentrations (ng m<sup>-3</sup>) of individual NACs in Q<sub>f</sub> and Q<sub>b</sub> samples by fuel type  
311 and WBT phase. The corresponding average mass ratios of individual NACs to OC × 100%  
312 (iNAC<sub>OC</sub>%) are ~~shown~~ exhibited in Fig. S2. Details of the NACs composition expressed in  
313 iNAC<sub>OC</sub>% for each fuel-cookstove experiment are given in Tables ~~S5S6-S8S9~~.

314 Generally, the CS and HS phases have consistent NAC profiles for red oak combustion  
315 (Figs. 1a, b and S2a, b). C<sub>10</sub>H<sub>7</sub>NO<sub>3</sub> (CS-Q<sub>f</sub> 1003 ± 803 ng m<sup>-3</sup>, HS-Q<sub>f</sub> 1149 ± 1053 ng m<sup>-3</sup>) and  
316 C<sub>8</sub>H<sub>5</sub>NO<sub>2</sub> (CS-Q<sub>f</sub> 712 ± 921 ng m<sup>-3</sup>, HS-Q<sub>f</sub> 1185 ± 1761 ng m<sup>-3</sup>) ~~has~~ have the highest average  
317 concentrations ~~(CS-Q<sub>f</sub> 1003 ± 803 ng m<sup>-3</sup>, HS-Q<sub>f</sub> 1149 ± 1053 ng m<sup>-3</sup>)~~ and iNAC<sub>OC</sub>% (CS-Q<sub>f</sub> 0.45  
318 ± 0.80%, HS-Q<sub>f</sub> 0.43 ± 0.79%) on Q<sub>f</sub>, followed by C<sub>11</sub>H<sub>9</sub>NO<sub>3</sub>, C<sub>10</sub>H<sub>11</sub>NO<sub>5</sub>, and C<sub>11</sub>H<sub>13</sub>NO<sub>5</sub>.  
319 However, C<sub>8</sub>H<sub>5</sub>NO<sub>2</sub> was only detected in emission samples of Jiko Poa among the five wood  
320 stoves (Tables S6 and S7). Not considering C<sub>8</sub>H<sub>5</sub>NO<sub>2</sub>, Q<sub>b</sub> samples of red oak combustion  
321 emissions have similar NACs profiles and characteristic species (e.g., C<sub>10</sub>H<sub>7</sub>NO<sub>3</sub>, C<sub>11</sub>H<sub>9</sub>NO<sub>3</sub>) as  
322 Q<sub>f</sub> samples, and the individual NAC distributions in Q<sub>b</sub> to Q<sub>f</sub> samples are similar between the CS-  
323 and HS-phases (Fig. 1a, b). It appears that the formation of NACs from red oak burning in  
324 cookstoves depends largely on burn conditions reflected by EC/OC ratios (Fig. S1c) rather than  
325 WBT phases. Among the 17 identified NACs from red oak burning, C<sub>8</sub>H<sub>5</sub>NO<sub>2</sub> and C<sub>11</sub>H<sub>13</sub>NO<sub>6</sub>

设置了格式: 下标

设置了格式: 下标

设置了格式: 下标

326 have the lowest  $Q_b$  to  $Q_f$  ratios (~~2.42-03~~ – ~~12.69.80~~%, Fig. 1a, b), indicating their low volatility.  
327 The low volatility of  $C_{11}H_{13}NO_6$  might be due to its relatively high MW; while  $C_8H_5NO_2$  has the  
328 second lowest MW and its structure likely contains functional groups that decrease vapor pressure  
329 (e.g., carboxyl group) (Donahue et al., 2011).

330 Charcoal burning generated high abundances of  $C_8H_9NO_5$ ,  $C_{11}H_9NO_3$ , and  $C_{10}H_7NO_3$  for  
331 both CS ( $86.6 \pm 98.7 - 170 \pm 200 \text{ ng m}^{-3}$ ) and HS ( $97.1 \pm 38.5 - 178 \pm 104 \text{ ng m}^{-3}$ ) phases (Figs.  
332 1c, d and S2c, d). Only one of the five charcoal stoves (Éclair, GIZ, Bonn, Germany) emitted  
333  $C_8H_5NO_2$ , which was not detected on  $Q_b$  for charcoal combustions (Tables S8 and S9). Average  
334 concentrations of  $C_8H_9NO_5$ ,  $C_{11}H_9NO_3$ , and  $C_{10}H_7NO_3$  in the  $Q_b$  ( $62.0 \pm 64.9 - 198 \pm 115 \text{ ng m}^{-3}$ )  
335 and  $Q_f$  samples were comparable. However, the iNAC<sub>OC</sub>% of these compounds are  $1.45 \pm 0.68 -$   
336  $5.16 \pm 2.84$  times higher in  $Q_b$  (iNAC<sub>OC</sub>%,  $0.11 \pm 0.18 - 0.46 \pm 0.69\%$ ) than in  $Q_f$  samples ( $0.052$   
337  $\pm 0.067 - 0.14 \pm 0.15\%$ ). High levels of  $C_6H_5NO_4$ ,  $C_7H_7NO_4$ , and  $C_8H_9NO_4$  were also observed in  
338 the HS phase for charcoal burning (Fig. 1d). These compounds in  $Q_b$  samples had average  
339 concentrations ( $222 \pm 132 - 297 \pm 277 \text{ ng m}^{-3}$ )  $22.6 - 80.8\%$  higher than in  $Q_f$  samples ( $150 \pm 118$   
340  $- 181 \pm 111 \text{ ng m}^{-3}$ ). As such, the charcoal HS phase generates more low MW NACs (e.g.,  
341  $C_6H_5NO_4$ ,  $C_7H_7NO_4$ ) than the CS phase, and the initial temperature in the cookstove has an impact  
342 on NAC formation from charcoal burning.

343 As mentioned in section 3.1, using a  $Q_b$  has been widely applied to evaluate the positive  
344 sampling artifact for OC and semivolatile organic compounds. This method might only work for  
345 bulk PM, OC, and low volatile organic compounds, of which the concentrations in  $Q_b$  samples are  
346 much lower than  $Q_f$  samples and usually presumed to be due to positive adsorption artifacts only  
347 (Subramanian et al., 2004; Watson et al., 2009). In this work, the average  $Q_b$  to  $Q_f$  mass ratios of  
348 the 17 individual NACs ranged from ~~54.350.8~~  $\pm$  ~~24.513.4~~% to ~~135-140~~  $\pm$  ~~52.49~~%, comparable to

设置了格式: 字体: (默认) Times New Roman, 12 磅

设置了格式: 下标

设置了格式: 下标

设置了格式: 下标

设置了格式: 字体: 倾斜, 下标



349 *n*-alkanes with carbon number  $\leq 21$  (e.g., hencosane; 26.3 – 163%) and PAHs with benzene ring  
350 number  $\leq 4$  (e.g., fluoranthene; 46.3 – 134%) in the ambient of urban Denver (Xie et al., 2014).  
351 Xie et al. (2014) found that the gas-phase concentrations of *n*-alkanes and PAHs with vapor  
352 pressure greater than hencosane and fluoranthene were comparable or higher than their particle-  
353 phase concentrations. The vapor pressure of five NACs standards at 25 °C ( $p^{o,*}_L$ ) were predicted  
354 using the US EPA Toxicity Estimation Software Tool (T.E.S.T) and listed in Table S10. Their  
355  $p^{o,*}_L$  values are mostly higher than hencosane and fluoranthene ( $\sim 10^{-8}$  atm; Xie et al., 2013, 2014).  
356 Then the identified NACs in this study may have substantial fractions remaining in the gas phase.  
357 ~~As and~~ the evaporation of NACs from  ~~$Q_f$~~  the upstream filter (negative artifact) is unknown. ~~As a~~  
358 ~~result,~~ the particle-phase NAC concentrations cannot be calculated by simply subtracting  $Q_b$   
359 measurements from those of  $Q_f$ . Considering that most of the  $Q_f$  and  $Q_b$  samples were collected  
360 near ambient temperature (Table S2,  $\sim 25$  °C), ~~some of the identified NACs (e.g., 4-nitrophenol)~~  
361 ~~may have substantial gas phase concentrations (Li et al., 2020), and~~ the composition of NACs  
362 derived from  $Q_f$  measurements alone can be biased due to the lack of gas-phase measurements.  
363 Future work is needed to evaluate the composition of NACs from emission sources in both the  
364 particle and gas phases.

### 365 3.3 Identification of NACs structures

366 Figures S3 and S4 exhibited extracted ion chromatograms (EICs) and MS-MS spectra of  
367 the 17 identified NACs. For comparison, the MS-MS spectra of standard compounds used in this  
368 work are obtained from Xie et al. (2017a, 2019) and shown in Fig. S5. Among all identified NAC  
369 formulas,  $C_{10}H_7NO_3$  was detected in each fuel-cookstove experiment (Tables ~~S5-S6~~ – ~~S8S9~~) and  
370 showed the highest concentrations in emissions from burning red oak (Fig. 1a, b). The MS-MS  
371 spectrum of  $C_{10}H_7NO_3$  (Fig. S4l) is like 2-nitro-1-phenol (Fig. S5g) but shows a  $\sim 1$  min difference

设置了格式: 上标

设置了格式: 非上标/ 下标

372 in retention time (Fig. S3i 10.9 min, 2-nitro-1-phenol 11.8 min).  $C_{10}H_7NO_3$  is presumed to be an  
373 isomer of 2-nitro-1-phenol with a nitronaphthol structure.  $C_{11}H_9NO_3$  has a degree of unsaturation  
374 and a fragmentation pattern (Fig. S4q) like  $C_{10}H_7NO_3$  and is likely a structural isomer of methyl  
375 nitronaphthol.  $C_6H_5NO_3$ ,  $C_7H_7NO_3$ ,  $C_6H_5NO_4$ , and  $C_7H_7NO_4$  are commonly detected in  
376 combustion emissions (Lin et al., 2016, 2017; Xie et al., ~~2017a~~2019) and atmospheric particles  
377 (Claeys et al., 2012; Zhang et al., 2013).  $C_6H_5NO_3$  and  $C_6H_5NO_4$  are identified as 4-nitrophenol  
378 and 4-nitrocatechol using authentic standards (Figs. S4a, d and S5a, c).  $C_7H_7NO_3$  has two isomers  
379 (Fig. S3b) and the compound eluting at 9.98 min has the same retention time and MS-MS spectrum  
380 (Fig. S4c) as 2-methyl-4-nitrophenol (Fig. S5b). In ambient PM and chamber SOA,  $C_7H_7NO_4$  was  
381 identified using standard compounds as a series of methyl-nitrocatechol isomers (4-methyl-5-  
382 nitrocatechol, 3-methyl-5-nitrocatechol, and 3-methyl-6-nitrocatechol) (Iinuma et al., 2010).  
383 According to the HPLC-Q-ToFMS data for  $C_7H_7NO_4$  identified in Iinuma et al. (2010) and our  
384 previous studies (Xie et al., 2017a, 2019), the two  $C_7H_7NO_4$  isomers in Fig. S3d are likely 4-  
385 methyl-5-nitrocatechol and 3-methyl-6-nitrocatechol, respectively. Here we cannot rule out the  
386 presence of 3-methyl-5-nitrocatechol, which may co-elute with 4-methyl-5-nitrocatechol (Iinuma  
387 et al., 2010). In Fig. S4k, o, and p, the MS-MS spectra of  $C_7H_7NO_5$ ,  $C_8H_7NO_5$ , and  $C_8H_9NO_5$  all  
388 show a loss of  $CH_3 + NO$  (or  $NO_2$ ) +  $CO$ . The loss of  $CH_3$  is typically due to a methoxy group in  
389 NAC molecules, and  $NO$  (or  $NO_2$ ) and  $CO$  loss is commonly observed for NACs with more than  
390 one phenoxy group (Xie et al., 2019). So methoxy nitrophenol is the proposed skeleton for  
391  $C_7H_7NO_5$ ,  $C_8H_7NO_5$ , and  $C_8H_9NO_5$ . Other functional groups were estimated using their chemical  
392 formulas and degree of unsaturation as a basis (Table S3).

393 The present study quantifies  $C_8H_7NO_4$  and  $C_9H_9NO_4$  using 2-methyl-5-benzoic acid  
394 ( $C_8H_7NO_4$ ) and 2,5-dimethyl-4-nitrobenzoic acid ( $C_9H_9NO_4$ ), respectively. The fragmentation

395 patterns of  $C_8H_7NO_4$  (Fig. S4g, h) and  $C_9H_9NO_4$  compounds (Fig. S4m, n) are different from their  
396 corresponding surrogates (Fig. S5f, h) and loss of  $CO_2$  is not observed, so  $C_8H_7NO_4$  and  $C_9H_9NO_4$   
397 compound structures do not include a carboxyl group. The MS-MS spectra of  $C_8H_7NO_4$  eluting at  
398 8.14 min (Fig. S3e) and  $C_9H_9NO_4$  eluting at 9.22 min (Fig. S3j) indicate the loss of OCN (Fig.  
399 S4g, m), suggesting benzoxazole/benzisoxazole structure or the presence of cyanate ( $-O-C\equiv N$ ) or  
400 isocyanate ( $-O=C=N$ ) groups. Mass spectra of selected standard compounds (Fig. S5i-n) in our  
401 previous work (Xie et al. 2019) show the loss of an OCN group only happens during the  
402 fragmentation of phenyl cyanate. Thus, the  $C_8H_7NO_4$  and  $C_9H_9NO_4$  isomers containing OCN  
403 indicate a phenyl cyanate feature. However, the fragmentation mechanism related to the loss of a  
404 single nitrogen for the second  $C_8H_7NO_4$  isomer (Figs. S3e, Fig. and S4h) is unknown and requires  
405 further study. The MS-MS spectrum of the second  $C_9H_9NO_4$  isomer had dominant ions at  $m/z$  194  
406 ( $[M-H]^+$ ), 164 (loss of NO), and 149 (loss of NO +  $CH_3$ ). Compared with the MS-MS spectra of  
407 4-nitrophenol and 2-methyl-4-nitrophenol (Fig. S5a, b), the second  $C_9H_9NO_4$  isomer is likely a  
408 methoxy nitrophenol with an extra ethyl group.

409 The EIC signal of  $C_8H_9NO_4$  in Fig. S3f comprises at least 3-4 isomers, and the MS-MS  
410 spectra are always dominated by ions at  $m/z$  182 ( $[M-H]^+$ ), 152 (loss of NO), and 137 (loss of NO  
411 +  $CH_3$ ) with some changes in relative abundance. The fragmentation mechanism of  $C_8H_9NO_4$   
412 represented by the MS-MS spectrum in Fig. S4i is consistent with that of the second  $C_9H_9NO_4$   
413 isomer (Fig. S4n), so the  $C_8H_9NO_4$  might also have a methoxy nitrophenol skeleton.

414 ~~Unlike other NACs,  $C_8H_5NO_2$  was only detected in samples from red oak burning in the Jiko Poa~~  
415 ~~and charcoal burning in the Éclair (Tables S5–S8). The average mass ratios of  $C_8H_5NO_2$  in  $Q_b$  to~~  
416  ~~$Q_f$  samples for red oak burning are less than 15% (CS phase 2.42%, HS phase 12.6%), and~~  
417  ~~$C_8H_5NO_2$  was not detected in any  $Q_b$  samples for charcoal burning.~~ The MS-MS spectrum of

带格式的: 缩进: 首行缩进: 0 厘米

418  $C_8H_5NO_2$  is characterized by  $CO_2$  loss (Fig. S4j), indicative of a carboxyl group. Considering the  
419 degree of unsaturation of the  $C_8H_5NO_2$  molecule and the cyano group feature in BB tracers (e.g.,  
420 hydrogen cyanide, benzonitrile) (Schneider et al., 1997; Li et al., 2000; Gilman et al., 2015),

421  $C_8H_5NO_2$  ~~was identified as~~ ~~may be a~~ 4-cyanobenzoic acid ~~using~~ ~~authentic standard~~ (Fig. S5o).

422 The  $C_{10}H_{11}NO_4$ ,  $C_{10}H_{11}NO_5$ ,  $C_{11}H_{13}NO_5$ , and  $C_{11}H_{13}NO_6$  detected here are also observed in other  
423 BB experiments (Xie et al., 2019). Their MS-MS spectra are characterized by the loss of at least  
424 one  $CH_3$  and/or  $OCN$  (Fig. S4r–u), suggestive of methoxy or cyanate groups. Without authentic  
425 standards, fragmentation patterns (Fig. S4r–u) were used to determine the molecular structures of  
426  $C_{10}H_{11}NO_4$ ,  $C_{10}H_{11}NO_5$ ,  $C_{11}H_{13}NO_5$ , and  $C_{11}H_{13}NO_6$  (Table S3).

427 Nearly all NAC formulas identified in this work were observed previously (Lin et al., 2016,  
428 2017; Xie et al., 2017a; Fleming et al., 2018; Xie et al., 2019). Few studies attempt to retrieve  
429 structural information for NACs using MS-MS spectra of authentic standards. Although multiple  
430 NACs may be generated from BB and photooxidation of aromatics in the presence of  $NO_x$ , NAC  
431 structures may differ across emission sources. Xie et al. (2019) found that fragmentation patterns  
432 of  $C_7H_7NO_5$  and  $C_8H_9NO_5$  from BB and photochemical reactions are distinct, and the methoxy  
433 and cyanate groups are featured only in BB NACs. Thus, knowing the NAC structure is useful to  
434 emissions source identification. In this work, the chemical and structural information obtained for  
435 NACs sampled during red oak and charcoal burning are similar, presumably because the charcoal  
436 fuel used is produced by the slow pyrolysis of wood. However, NACs in red oak and charcoal  
437 burning emissions can be differentiated compositionally. As shown in Figs. 1 and S2, the NAC  
438 emissions from red oak burning in cookstoves are characterized by  $C_{10}H_7NO_3$  and  $C_{11}H_9NO_3$ . In  
439 addition to these two species, charcoal burning in cookstoves also generates high fractions of  
440  $C_8H_9NO_5$  (Fig. S2c, d). This difference among NACs may help with source apportionment ~~using~~

441 receptor models, which are commonly used and assume that the ambient pollutants measured in  
442 the field are linear combinations from a number of time-variant sources/factors. (Jaekels et al.,  
443 2007; Shrivastava et al., 2007; Xie et al., 2013).

444 Figure 2 compares NAC composition from cookstove emissions (not including C<sub>8</sub>H<sub>5</sub>NO<sub>2</sub>),  
445 open BB (Xie et al., 2019), and SOA chamber experiments (Xie et al., 2017a). Since previous  
446 source emissions studies ignored Q<sub>b</sub> measurements and normalized individual NACs  
447 concentrations to OM, only Q<sub>f</sub> measurements in this work are compared (Fig. 2a, b) with their  
448 iNACoc% values multiplied by 1.7 (proposed OM/OC ratio, Reff et al., 2009). The three open BB  
449 tests (Fig. 2c) were conducted with two fuel types under different ambient temperatures (10–29  
450 °C) and RH% (49–83%) (Xie et al., 2019). But they consistently emit C<sub>6</sub>H<sub>5</sub>NO<sub>4</sub>, C<sub>7</sub>H<sub>7</sub>NO<sub>4</sub>, and  
451 C<sub>9</sub>H<sub>9</sub>NO<sub>4</sub>, which is compositionally distinct from cookstove emissions (Fig. 2a, b). Moreover, the  
452 average mass contribution of total NACs to OM for open BB (0.12 ± 0.051%) was 4–14 times  
453 lower than that for cookstove emissions. This result is likely due to the high temperature flaming  
454 combustion produced in the cookstoves (Shen et al., 2012; Xie et al., 2018). In Fig. 2d and e, the  
455 NAC profiles yielded for photochemical reactions appear to have aromatic precursors. When using  
456 field measurement data of NACs for receptor modeling, the resulting factors can be linked with  
457 specific emission sources by comparing with the NAC patterns shown in Fig. 2. Further studies  
458 are also warranted to unveil NAC patterns of other potential sources (e.g., motor vehicle emissions).  
459 Therefore, the source of NACs can be identified by combining their characteristic structures and  
460 composition. The filter-based NACs reported for the experiments shown in ~~Figure~~ Fig. 2 were all  
461 measured using the identical method and HPLC-Q-ToFMS instrument, reducing any potential  
462 methodological bias. However, total gas-phase NAC concentrations need to be properly sampled  
463 and measured to account for the impact of gas/particle partitioning on their distribution.

设置了格式: 下标

设置了格式: 下标

设置了格式: 下标

#### 464 3.4 Contributions of NACs to Abs<sub>365</sub>

465 The average Abs<sub>365,tNAC</sub>% values of Q<sub>f</sub> and Q<sub>b</sub> samples are presented by fuel type and WBT  
466 phase in the Fig. 3 stack plots, and experimental data for each fuel-cookstove are provided in  
467 Tables ~~S9S11–S12S14~~. The average contributions of total NACs to Abs<sub>365</sub> (Abs<sub>365,tNAC</sub>%) of the  
468 sample extracts (Q<sub>f</sub> 1.10 – 2.5857%, Q<sub>b</sub> 10.7 – 21.0%) are up to 10 times greater than their average  
469 tNAC<sub>OC</sub>% (Q<sub>f</sub> 0.31 – 0.971.01%, Q<sub>b</sub> 1.08 – 3.31%, Table 1). Considering that some NACs are not  
470 light-absorbing (Table S4) and the OM/OC ratio is typically greater than unity, most NACs that  
471 contribute to Abs<sub>365</sub> are strong BrC chromophores. Like the mass composition of NACs (Fig. 1),  
472 C<sub>10</sub>H<sub>7</sub>NO<sub>3</sub> (CS 0.24%, HS 0.43%) and C<sub>8</sub>H<sub>9</sub>NO<sub>5</sub> (CS 1.22%, HS 0.55%) were the major  
473 contributors to Abs<sub>365</sub> for the Q<sub>f</sub> samples collected during red oak and charcoal burning,  
474 respectively (Fig.3a). The average Abs<sub>365,tNAC</sub>% of Q<sub>b</sub> samples are 7.53 to 11.3 times higher than  
475 those of Q<sub>f</sub> samples. Unlike the Q<sub>f</sub> samples from red oak burning, C<sub>10</sub>H<sub>11</sub>NO<sub>5</sub> (CS 2.77%, HS  
476 3.09%) has the highest average contribution to Abs<sub>365</sub> for Q<sub>b</sub> samples, followed by C<sub>10</sub>H<sub>7</sub>NO<sub>3</sub> (CS  
477 1.96%, HS 1.32%) and C<sub>8</sub>H<sub>9</sub>NO<sub>5</sub> (CS 1.32%, HS 1.44%). While C<sub>8</sub>H<sub>9</sub>NO<sub>5</sub> dominated the  
478 contribution (CS 8.78%, HS 5.82%) to Abs<sub>365</sub> for the Q<sub>b</sub> samples from charcoal burning (Fig. 3b).  
479 However, the All identified NACs only explained a minor fraction (<5%) 1.10 – 2.58% (Fig. S3)  
480 of Q<sub>b</sub> bulk extracts absorption. Even if the NACs on Q<sub>b</sub> were totally derived from upstream filter  
481 evaporation, the adjusted average contributions of total NACs (Q<sub>f</sub> + Q<sub>b</sub>) to Abs<sub>365</sub> of Q<sub>f</sub> extracts  
482 were still lower than 5% (1.59 – 4.01%). Due to the lack of authentic standards, the quantification  
483 of NACs concentrations and their contributions to Abs<sub>365</sub> of Q<sub>f</sub> extracts might be subject to  
484 uncertainties. However, growing evidences showed that BrC absorption was majorly contributed  
485 by large molecules with MW > 500 – 1000 Da (Di Lorenzo and Young, 2016; Di Lorenzo et al.,  
486 2017). Large molecules of NACs may be generated from flaming combustions in cookstoves, and

设置了格式: 字体: 倾斜, 下标

487 ~~their structures and light absorption are worth future investigations. Chen and Bond (2010)~~  
488 ~~hypothesized that BrC absorption is strongly associated with large molecules containing~~  
489 ~~conjugated aromatic rings and functional groups. Additionally, Di Lorenzo et al. (2017)~~  
490 ~~demonstrated that the majority of BrC absorption arises from large molecules with MW > 500~~  
491 ~~4000 Da. In previous studies on ambient and biomass burning particles, most identified NACs had~~  
492 ~~a MW lower than 300 – 500 Da, and their total contributions to bulk BrC absorption were estimated~~  
493 ~~to be less than 10% (Mohr et al., 2013; Zhang et al., 2013; Teich et al., 2017; Xie et al., 2019).~~  
494 ~~Similar results were also obtained in the current work. Therefore, further studies are needed to~~  
495 ~~identify large BrC molecules (including high MW NACs) in ambient and source particles. In~~  
496 ~~previous studies, less than 10% of the BrC absorption at  $\lambda = 365$  nm from ambient or BB particles~~  
497 ~~are ascribed to NACs with MW < 300 Da. Further studies are needed to identify these larger~~  
498 ~~molecules that are the dominant light absorbers in BB and cookstove PM. The average  $Abs_{365, NAC}$~~   
499 ~~of  $Q_b$  samples are 7.52 to 11.3 times higher than those of  $Q_f$  samples. Unlike the  $Q_f$  samples from~~  
500 ~~red oak burning,  $C_{10}H_{11}NO_3$  (CS 2.77%, HS 3.09%) has the highest average contribution to  $Abs_{365}$~~   
501 ~~for  $Q_b$  samples, followed by  $C_{10}H_7NO_3$  (CS 1.96%, HS 1.32%) and  $C_8H_9NO_5$  (CS 1.32%, HS~~  
502 ~~1.44%). While  $C_8H_9NO_5$  dominated the contribution (CS 8.78%, HS 5.82%) to  $Abs_{365}$  for the  $Q_b$~~   
503 ~~samples from charcoal burning (Fig. 3b). As mentioned in section 3.2, some NACs identified in~~  
504 ~~this work might have substantial gas phase concentrations. Jacobson (1999) inferred that the~~  
505 ~~nitrate-bearing aromatic gases may play a role in reducing the UV irradiance within the boundary~~  
506 ~~layer in Los Angeles during 1973 – 1987. Therefore, we suspect that gaseous NACs may be an~~  
507 ~~important group of molecules absorbing in short UV region in the atmosphere.~~

#### 508 **4 Conclusion**



509 This study investigated the composition, chemical formulas, and structures of NACs in  
510 PM<sub>2.5</sub> emitted from burning red oak and charcoal in a variety of cookstoves. Total NAC mass and  
511 compositional differences between Q<sub>f</sub> and Q<sub>b</sub> samples suggest that the identified NACs might have  
512 substantial gas-phase concentrations. By comparing the MS-MS spectra of identified NACs to  
513 standard compound spectra, the structures of NACs featuring methoxy and cyanate groups in  
514 cookstove emissions are confirmed. The source identification of NACs would be less ambiguous  
515 if both the structures and composition of NACs are known, as different emission sources have  
516 distinct NAC characteristics. However, the compositional information of NACs based on Q<sub>f</sub>  
517 measurements only are biased due to the lack of gas-phase data, and further studies are warranted  
518 to investigate the gas/particle distribution of NACs in the ambient and source emissions. Similar  
519 to previous work, the average contribution of total NACs to Abs<sub>365</sub> of Q<sub>f</sub> samples is less than 5%  
520 (1.10 – 2.5857%), suggesting the need to shift our focus from low MW NACs (MW < 300 Da) to  
521 the chemical and optical properties of large molecules (e.g., MW > 500 Da) in particles. ~~However,~~  
522 ~~their average contributions to Abs<sub>365</sub> of Q<sub>b</sub> samples are 7.52 to 11.3 times higher, so NACs may~~  
523 ~~be important light absorbers in the gas phase. Further research in understanding the influence of~~  
524 ~~gaseous chromophores on the earth's radiative balance is warranted.~~

设置了格式: 字体: 倾斜, 下标

#### 526 ***Data availability***

527 Data used in the writing of this manuscript is available at the U.S. Environmental Protection  
528 Agency's Environmental Dataset Gateway (<https://edg.epa.gov>).

#### 530 ***Competing interests***

531 The authors declare that they have no conflict of interest.

532

533 **Disclaimer**

534 The views expressed in this article are those of the authors and do not necessarily represent the  
535 views or policies of the U.S. Environmental Protection Agency.

536

537 **Author contribution**

538 MX and AH designed the research. MX, ZZ, and XC performed the experiments. GS, [WC](#), and JJ  
539 managed [cookstove emission tests and](#) sample collection. MX and MH analyzed the data and wrote  
540 the paper with significant contributions from AH and QW.

541

542 **Acknowledgements**

543 This research was supported by the National Natural Science Foundation of China (NSFC,  
544 41701551), the Startup Foundation for Introducing Talent of NUIST (No. 2243141801001), and  
545 in part by an appointment to the Postdoctoral Research Program at the Office of Research and  
546 Development by the Oak Ridge institute for Science and Education through Interagency  
547 Agreement No. 92433001 between the U.S. Department of Energy and the U.S. Environmental  
548 Protection Agency. We thank B. Patel for assistance on ECOC analysis of PM<sub>2.5</sub> filters.

549

550 **References**

551 [Ahrens, L., Harner, T., Shoeib, M., Lane, D. A., and Murphy, J. G.: Improved characterization of gas-particle](#)  
552 [partitioning for per- and polyfluoroalkyl substances in the atmosphere using annular diffusion denuder samplers,](#)  
553 [Environmental Science & Technology, 46, 7199-7206, 10.1021/es300898s, 2012.](#)  
554 Anenberg, S. C., Balakrishnan, K., Jetter, J., Masera, O., Mehta, S., Moss, J., and Ramanathan, V.: Cleaner cooking  
555 solutions to achieve health, climate, and economic cobenefits, *Environmental Science & Technology*, 47, 3944-  
556 3952, 10.1021/es304942e, 2013.  
557 Aunan, K., Berntsen, T. K., Myhre, G., Rypdal, K., Streets, D. G., Woo, J.-H., and Smith, K. R.: Radiative forcing  
558 from household fuel burning in Asia, *Atmospheric Environment*, 43, 5674-5681,  
559 <https://doi.org/10.1016/j.atmosenv.2009.07.053>, 2009.

560 Bond, T. C., Streets, D. G., Yarber, K. F., Nelson, S. M., Woo, J.-H., and Klimont, Z.: A technology-based global  
561 inventory of black and organic carbon emissions from combustion, *Journal of Geophysical Research:*  
562 *Atmospheres*, 109, 10.1029/2003jd003697, 2004.

563 Bonjour, S., Adair-Rohani, H., Wolf, J., Bruce Nigel, G., Mehta, S., Prüss-Ustün, A., Lahiff, M., Rehfues Eva, A.,  
564 Mishra, V., and Smith Kirk, R.: Solid fuel use for household cooking: Country and regional estimates for 1980–  
565 2010, *Environmental Health Perspectives*, 121, 784-790, 10.1289/ehp.1205987, 2013.

566 Cao, G., Zhang, X., and Zheng, F.: Inventory of black carbon and organic carbon emissions from China, *Atmospheric*  
567 *Environment*, 40, 6516-6527, <https://doi.org/10.1016/j.atmosenv.2006.05.070>, 2006.

568 Chen, Y., Sheng, G., Bi, X., Feng, Y., Mai, B., and Fu, J.: Emission ~~Factors~~-factors for carbonaceous particles and  
569 polycyclic aromatic hydrocarbons from residential coal combustion in China, *Environmental Science &*  
570 *Technology*, 39, 1861-1867, 10.1021/es0493650, 2005.

571 Chen, Y., and Bond, T. C.: Light absorption by organic carbon from wood combustion, *Atmospheric Chemistry and*  
572 *Physics*, 10, 1773-1787, 10.5194/acp-10-1773-2010, 2010.

573 Claeys, M., Vermeylen, R., Yasmeen, F., Gómez-González, Y., Chi, X., Maenhaut, W., Mészáros, T., and Salma, I.:  
574 Chemical characterisation of humic-like substances from urban, rural and tropical biomass burning environments  
575 using liquid chromatography with UV/vis photodiode array detection and electrospray ionisation mass  
576 spectrometry, *Environmental Chemistry*, 9, 273-284, <https://doi.org/10.1071/EN11163>, 2012.

577 De Haan, D. O., Hawkins, L. N., Welsh, H. G., Pednekar, R., Casar, J. R., Pennington, E. A., de Loera, A., Jimenez,  
578 N. G., Symons, M. A., Zauscher, M., Pajunoja, A., Caponi, L., Cazaunau, M., Formenti, P., Gratien, A., Pangui,  
579 E., and Doussin, J.-F.: Brown carbon production in ammonium- or amine-containing aerosol particles by reactive  
580 uptake of methylglyoxal and photolytic cloud cycling, *Environmental Science & Technology*, 51, 7458-7466,  
581 10.1021/acs.est.7b00159, 2017.

582 Desyaterik, Y., Sun, Y., Shen, X., Lee, T., Wang, X., Wang, T., and Collett, J. L.: Speciation of “brown” carbon in  
583 cloud water impacted by agricultural biomass burning in eastern China, *Journal of Geophysical Research:*  
584 *Atmospheres*, 118, 7389-7399, 10.1002/jgrd.50561, 2013.

585 [Ding, Y., Pang, Y., and Eatough, D. J.: High-volume diffusion denuder sampler for the routine monitoring of fine  
586 particulate matter: I. Design and optimization of the PC-BOSS, \*Aerosol Science and Technology\*, 36, 369-382,  
587 10.1080/027868202753571205, 2002.](#)

588 [Di Lorenzo, R. A., and Young, C. J.: Size separation method for absorption characterization in brown carbon:  
589 Application to an aged biomass burning sample, \*Geophysical Research Letters\*, 43, 458-465,  
590 10.1002/2015gl066954, 2016.](#)

591 Di Lorenzo, R. A., Washenfelder, R. A., Attwood, A. R., Guo, H., Xu, L., Ng, N. L., Weber, R. J., Baumann, K.,  
592 Edgerton, E., and Young, C. J.: Molecular-size-separated brown carbon absorption for biomass-burning aerosol  
593 at multiple field sites, *Environmental Science & Technology*, 51, 3128-3137, 10.1021/acs.est.6b06160, 2017.

594 Donahue, N. M., Epstein, S. A., Pandis, S. N., and Robinson, A. L.: A two-dimensional volatility basis set: 1.  
595 organic-aerosol mixing thermodynamics, *Atmospheric Chemistry and Physics*, 11, 3303-3318, 10.5194/acp-11-  
596 3303-2011, 2011.

597 Feng, Y., Ramanathan, V., and Kotamarthi, V. R.: Brown carbon: a significant atmospheric absorber of solar  
598 radiation?, *Atmospheric Chemistry and Physics*, 13, 8607-8621, 10.5194/acp-13-8607-2013, 2013.

599 Fleming, L. T., Lin, P., Laskin, A., Laskin, J., Weltman, R., Edwards, R. D., Arora, N. K., Yadav, A., Meinardi, S.,  
600 Blake, D. R., Pillarisetti, A., Smith, K. R., and Nizkorodov, S. A.: Molecular composition of particulate matter  
601 emissions from dung and brushwood burning household cookstoves in Haryana, India, *Atmospheric Chemistry*  
602 *and Physics*, 18, 2461-2480, 10.5194/acp-18-2461-2018, 2018.

603 Forrister, H., Liu, J., Scheuer, E., Dibb, J., Ziemba, L., Thornhill, K. L., Anderson, B., Diskin, G., Perring, A. E.,  
604 Schwarz, J. P., Campuzano-Jost, P., Day, D. A., Palm, B. B., Jimenez, J. L., Nenes, A., and Weber, R. J.: Evolution  
605 of brown carbon in wildfire plumes, *Geophysical Research Letters*, 42, 4623-4630, 10.1002/2015gl063897, 2015.

606 Gilman, J. B., Lerner, B. M., Kuster, W. C., Goldan, P. D., Warneke, C., Veres, P. R., Roberts, J. M., de Gouw, J. A.,  
607 Burling, I. R., and Yokelson, R. J.: Biomass burning emissions and potential air quality impacts of volatile organic  
608 compounds and other trace gases from fuels common in the US, *Atmospheric Chemistry and Physics*, 15, 13915-  
609 13938, 10.5194/acp-15-13915-2015, 2015.

610 Glarborg, P., Jensen, A., and Johnsson, J. E.: Fuel nitrogen conversion in solid fuel fired systems, *Progress in Energy*  
611 *and Combustion Science*, 29, 89-113, 2003.

612 Global Alliance for Clean Cookstoves, 2014. Water Boiling Test (WBT) 4.2.3. Released 19 March 2014  
613 <http://cleancookstoves.org/technology-and-fuels/testing/protocols.html> (accessed July 2017).

614 Harrison, M. A., Barra, S., Borghesi, D., Vione, D., Arsene, C., and Olariu, R. I.: Nitrated phenols in the atmosphere:  
615 a review, *Atmospheric Environment*, 39, 231-248, 2005.

616 Hecobian, A., Zhang, X., Zheng, M., Frank, N., Edgerton, E. S., and Weber, R. J.: Water-Soluble-soluble Organic  
617 organic Aerosol-aerosol material and the light-absorption characteristics of aqueous extracts measured over the  
618 Southeastern United States, *Atmospheric Chemistry and Physics*, 10, 5965-5977, 10.5194/acp-10-5965-2010,  
619 2010.

620 Iinuma, Y., Böge, O., Gräfe, R., and Herrmann, H.: Methyl-nitrocatechols: Atmospheric tracer compounds for  
621 biomass burning secondary organic aerosols, *Environmental Science & Technology*, 44, 8453-8459,  
622 10.1021/es102938a, 2010.

623 International Agency for Research on Cancer (IARC): Some non-heterocyclic polycyclic aromatic hydrocarbons and  
624 some related exposures (Vol. 92). IARC Press, International Agency for Research on Cancer, 2010.

625 Jacobson, M. Z.: Isolating nitrated and aromatic aerosols and nitrated aromatic gases as sources of ultraviolet light  
626 absorption, *Journal of Geophysical Research: Atmospheres*, 104, 3527-3542, 10.1029/1998jd100054, 1999.

627 Jaekels, J. M., Bae, M. S., and Schauer, J. J.: Positive matrix factorization (PMF) analysis of molecular marker  
628 measurements to quantify the sources of organic aerosols, *Environmental Science & Technology*, 41, 5763-5769,  
629 10.1021/es062536b, 2007.

630 Jetter, J. J., and Kariher, P.: Solid-fuel household cook stoves: Characterization of performance and emissions,  
631 *Biomass and Bioenergy*, 33, 294-305, <http://dx.doi.org/10.1016/j.biombioe.2008.05.014>, 2009.

632 Jetter, J., Zhao, Y., Smith, K. R., Khan, B., Yelverton, T., DeCarlo, P., and Hays, M. D.: Pollutant emissions and  
633 energy efficiency under controlled conditions for household biomass cookstoves and implications for metrics  
634 useful in setting international test standards, *Environmental Science & Technology*, 46, 10827-10834,  
635 10.1021/es301693f, 2012.

636 Kaal, J., Martínez Cortizas, A., and Nierop, K. G. J.: Characterisation of aged charcoal using a coil probe pyrolysis-  
637 GC/MS method optimised for black carbon, *Journal of Analytical and Applied Pyrolysis*, 85, 408-416,  
638 <https://doi.org/10.1016/j.jaap.2008.11.007>, 2009.

639 Kim, K.-H., Jahan, S. A., Kabir, E., and Brown, R. J. C.: A review of airborne polycyclic aromatic hydrocarbons  
640 (PAHs) and their human health effects, *Environment International*, 60, 71-80,  
641 <https://doi.org/10.1016/j.envint.2013.07.019>, 2013.

642 Kim Oanh, N. T., Bætz Reutergårdh, L., and Dung, N. T.: Emission of polycyclic aromatic hydrocarbons and  
643 particulate matter from domestic combustion of selected fuels, *Environmental Science & Technology*, 33, 2703-  
644 2709, 10.1021/es980853f, 1999.

645 Kirchstetter, T. W., Corrigan, C. E., and Novakov, T.: Laboratory and field investigation of the adsorption of gaseous  
646 organic compounds onto quartz filters, *Atmospheric Environment*, 35, 1663-1671, [https://doi.org/10.1016/S1352-2310\(00\)00448-9](https://doi.org/10.1016/S1352-2310(00)00448-9), 2001.

647 Klimont, Z., Cofala, J., Xing, J., Wei, W., Zhang, C., Wang, S., Kejun, J., Bhandari, P., Mathur, R., Purohit, P., Rafaj,  
648 P., Chambers, A., Amann, M., and Hao, J.: Projections of SO<sub>2</sub>, NO<sub>x</sub> and carbonaceous aerosols emissions in  
649 Asia, *Tellus B*, 61, 602-617, 10.1111/j.1600-0889.2009.00428.x, 2009.

650 Kwamena, N.-O., and Abbatt, J.: Heterogeneous nitration reactions of polycyclic aromatic hydrocarbons and n-hexane  
651 soot by exposure to NO<sub>3</sub>/NO<sub>2</sub>/N<sub>2</sub>O<sub>5</sub>, *Atmospheric Environment*, 42, 8309-8314, 2008.

652 Lacey, F., and Henze, D.: Global climate impacts of country-level primary carbonaceous aerosol from solid-fuel  
653 cookstove emissions, *Environmental Research Letters*, 10, 114003, 10.1088/1748-9326/10/11/114003, 2015.

654 Lei, Y., Zhang, Q., He, K. B., and Streets, D. G.: Primary anthropogenic aerosol emission trends for China, 1990-  
655 2005, *Atmos. Chem. Phys.*, 11, 931-954, 10.5194/acp-11-931-2011, 2011.

656 Li, M., Wang, X., Lu, C., Li, R., Zhang, J., Dong, S., Yang, L., Xue, L., Chen, J., and Wang, W.: Nitrated phenols  
657 and the phenolic precursors in the atmosphere in urban Jinan, China, *Science of The Total Environment*, 136760,  
658 <https://doi.org/10.1016/j.scitotenv.2020.136760>, 2020.

659 Li, Q., Jacob, D. J., Bey, I., Yantosca, R. M., Zhao, Y., Kondo, Y., and Notholt, J.: Atmospheric hydrogen cyanide  
660 (HCN): Biomass burning source, ocean sink?, *Geophysical Research Letters*, 27, 357-360,  
661 10.1029/1999gl10935, 2000.

662 Lin, P., Aiona, P. K., Li, Y., Shiraiwa, M., Laskin, J., Nizkorodov, S. A., and Laskin, A.: Molecular characterization  
663 of brown carbon in biomass burning aerosol particles, *Environmental Science & Technology*, 50, 11815-11824,  
664 10.1021/acs.est.6b03024, 2016.

665 Lin, P., Bluvshstein, N., Rudich, Y., Nizkorodov, S. A., Laskin, J., and Laskin, A.: Molecular chemistry of atmospheric  
666 brown carbon inferred from a nationwide biomass burning event, *Environmental Science & Technology*, 51,  
667 11561-11570, 10.1021/acs.est.7b02276, 2017.

668 Lin, P., Liu, J. M., Shilling, J. E., Kathmann, S. M., Laskin, J., and Laskin, A.: Molecular characterization of brown  
669 carbon (BrC) chromophores in secondary organic aerosol generated from photo-oxidation of toluene, *Physical  
670 Chemistry Chemical Physics*, 17, 23312-23325, 10.1039/c5cp02563j, 2015.

672 Liu, J., Bergin, M., Guo, H., King, L., Kotra, N., Edgerton, E., and Weber, R. J.: Size-resolved measurements of brown  
673 carbon in water and methanol extracts and estimates of their contribution to ambient fine-particle light absorption,  
674 *Atmospheric Chemistry and Physics*, 13, 12389-12404, 10.5194/acp-13-12389-2013, 2013.

675 Lu, C., Wang, X., Li, R., Gu, R., Zhang, Y., Li, W., Gao, R., Chen, B., Xue, L., and Wang, W.: Emissions of fine  
676 particulate nitrated phenols from residential coal combustion in China, *Atmospheric Environment*, 203, 10-17,  
677 <https://doi.org/10.1016/j.atmosenv.2019.01.047>, 2019.

678 Lu, J. W., Flores, J. M., Lavi, A., Abo-Riziq, A., and Rudich, Y.: Changes in the optical properties of benzo[a]pyrene-  
679 coated aerosols upon heterogeneous reactions with NO<sub>2</sub> and NO<sub>3</sub>, *Physical Chemistry Chemical Physics*, 13,  
680 6484-6492, 10.1039/C0CP02114H, 2011.

681 Lu, Z., Streets, D. G., Winijkul, E., Yan, F., Chen, Y., Bond, T. C., Feng, Y., Dubey, M. K., Liu, S., Pinto, J. P., and  
682 Carmichael, G. R.: Light absorption properties and radiative effects of primary organic aerosol emissions,  
683 *Environmental Science & Technology*, 49, 4868-4877, 10.1021/acs.est.5b00211, 2015.

684 McMeeking, G., Fortner, E., Onasch, T., Taylor, J., Flynn, M., Coe, H., and Kreidenweis, S.: Impacts of nonrefractory  
685 material on light absorption by aerosols emitted from biomass burning, *Journal of Geophysical Research: Atmospheres*,  
686 119, 12,272-212,286, 2014.

687 [Mohr, C., Lopez-Hilfiker, F. D., Zotter, P., Prévôt, A. S. H., Xu, L., Ng, N. L., Herndon, S. C., Williams, L. R.,  
688 Franklin, J. P., Zahniser, M. S., Worsnop, D. R., Knighton, W. B., Aiken, A. C., Gorkowski, K. J., Dubey, M. K.,  
689 Allan, J. D., and Thornton, J. A.: Contribution of nitrated phenols to wood burning brown carbon light absorption  
690 in Detling, United Kingdom during winter time, \*Environmental Science & Technology\*, 47, 6316-6324,  
691 \[10.1021/es400683v\]\(https://doi.org/10.1021/es400683v\), 2013.](https://doi.org/10.1021/es400683v)

692 Nakayama, T., Matsumi, Y., Sato, K., Imamura, T., Yamazaki, A., and Uchiyama, A.: Laboratory studies on optical  
693 properties of secondary organic aerosols generated during the photooxidation of toluene and the ozonolysis of  $\alpha$ -  
694 pinene, *Journal of Geophysical Research: Atmospheres*, 115, n/a-n/a, 10.1029/2010jd014387, 2010.

695 Park, R. J., Kim, M. J., Jeong, J. I., Youn, D., and Kim, S.: A contribution of brown carbon aerosol to the aerosol  
696 light absorption and its radiative forcing in East Asia, *Atmospheric Environment*, 44, 1414-1421,  
697 <https://doi.org/10.1016/j.atmosenv.2010.01.042>, 2010.

698 Peters, A. J., Lane, D. A., Gundel, L. A., Northcott, G. L., and Jones, K. C.: A comparison of high volume and diffusion  
699 denuder samplers for measuring semivolatile organic compounds in the atmosphere, *Environmental Science &  
700 Technology*, 34, 5001-5006, 10.1021/es000056t, 2000.

701 Pokhrel, R. P., Wagner, N. L., Langridge, J. M., Lack, D. A., Jayarathne, T., Stone, E. A., Stockwell, C. E., Yokelson,  
702 R. J., and Murphy, S. M.: Parameterization of single-scattering albedo (SSA) and absorption Ångström exponent  
703 (AAE) with EC/OC for aerosol emissions from biomass burning, *Atmospheric Chemistry and Physics*, 16, 9549-  
704 9561, 10.5194/acp-16-9549-2016, 2016.

705 Ravindra, K., Sokhi, R., and Van Grieken, R.: Atmospheric polycyclic aromatic hydrocarbons: Source attribution,  
706 emission factors and regulation, *Atmospheric Environment*, 42, 2895-2921,  
707 <https://doi.org/10.1016/j.atmosenv.2007.12.010>, 2008.

708 Reff, A., Bhawe, P. V., Simon, H., Pace, T. G., Pouliot, G. A., Mobley, J. D., and Houyoux, M.: Emissions inventory  
709 of PM<sub>2.5</sub> trace elements across the United States, *Environmental Science & Technology*, 43, 5790-5796,  
710 [10.1021/es802930x](https://doi.org/10.1021/es802930x), 2009.

711 Riddle, S. G., Jakober, C. A., Robert, M. A., Cahill, T. M., Charles, M. J., and Kleeman, M. J.: Large PAHs detected  
712 in fine particulate matter emitted from light-duty gasoline vehicles, *Atmospheric Environment*, 41, 8658-8668,  
713 <https://doi.org/10.1016/j.atmosenv.2007.07.023>, 2007.

714 Saleh, R., Robinson, E. S., Tkacik, D. S., Ahern, A. T., Liu, S., Aiken, A. C., Sullivan, R. C., Presto, A. A., Dubey,  
715 M. K., Yokelson, R. J., Donahue, N. M., and Robinson, A. L.: Brownness of organics in aerosols from biomass  
716 burning linked to their black carbon content, *Nature Geoscience*, 7, 647-650, 10.1038/ngeo2220, 2014.

717 Samburova, V., Connolly, J., Gyawali, M., Yatavelli, R. L. N., Watts, A. C., Chakrabarty, R. K., Zielinska, B.,  
718 Moosmüller, H., and Khlystov, A.: Polycyclic aromatic hydrocarbons in biomass-burning emissions and their  
719 contribution to light absorption and aerosol toxicity, *Science of The Total Environment*, 568, 391-401,  
720 <http://doi.org/10.1016/j.scitotenv.2016.06.026>, 2016.

721 Schneider, J., Bürger, V., and Arnold, F.: Methyl cyanide and hydrogen cyanide measurements in the lower  
722 stratosphere: Implications for methyl cyanide sources and sinks, *Journal of Geophysical Research: Atmospheres*,  
723 102, 25501-25506, 10.1029/97jd02364, 1997.

724 Shen, G., Tao, S., Wei, S., Zhang, Y., Wang, R., Wang, B., Li, W., Shen, H., Huang, Y., Chen, Y., Chen, H., Yang,  
725 Y., Wang, W., Wei, W., Wang, X., Liu, W., Wang, X., and Simonich, S. L. M.: Reductions in Emissions of  
726 Carbonaceous particulate matter and polycyclic aromatic hydrocarbons from combustion of biomass pellets in

727 comparison with raw fuel burning, *Environmental Science & Technology*, 46, 6409-6416, 10.1021/es300369d,  
728 2012.

729 Shrivastava, M. K., Subramanian, R., Rogge, W. F., and Robinson, A. L.: Sources of organic aerosol: Positive matrix  
730 factorization of molecular marker data and comparison of results from different source apportionment models,  
731 *Atmospheric Environment*, 41, 9353-9369, 10.1016/j.atmosenv.2007.09.016, 2007.

732 Simoneit, B. R., Rogge, W., Mazurek, M., Standley, L., Hildemann, L., and Cass, G.: Lignin pyrolysis products,  
733 lignans, and resin acids as specific tracers of plant classes in emissions from biomass combustion, *Environmental  
734 science & technology*, 27, 2533-2541, 1993.

735 Simoneit, B. R.: Biomass burning—a review of organic tracers for smoke from incomplete combustion, *Applied  
736 Geochemistry*, 17, 129-162, 2002.

737 Smith, K. R., Bruce, N., Balakrishnan, K., Adair-Rohani, H., Balmes, J., Chafe, Z., Dherani, M., Hosgood, H. D.,  
738 Mehta, S., Pope, D., and Rehfuess, E.: Millions dead: How do we know and what does it mean? Methods used in  
739 the comparative risk assessment of household air pollution, *Annual Review of Public Health*, 35, 185-206,  
740 10.1146/annurev-publhealth-032013-182356, 2014.

741 Subramanian, R., Khlystov, A. Y., Cabada, J. C., and Robinson, A. L.: Positive and negative artifacts in particulate  
742 organic carbon measurements with denuded and undenuded sampler configurations special issue of *Aerosol  
743 Science and Technology* on findings from the fine particulate matter supersites program, *Aerosol Science and  
744 Technology*, 38, 27-48, 10.1080/02786820390229354, 2004.

745 Sun, J., Zhi, G., Hitznerberger, R., Chen, Y., Tian, C., Zhang, Y., Feng, Y., Cheng, M., Cai, J., Chen, F., Qiu, Y., Jiang,  
746 Z., Li, J., Zhang, G., and Mo, Y.: Emission factors and light absorption properties of brown carbon from household  
747 coal combustion in China, *Atmospheric Chemistry and Physics*, 17, 4769-4780, 10.5194/acp-17-4769-2017, 2017.

748 Teich, M., van Pinxteren, D., Wang, M., Kecorius, S., Wang, Z., Müller, T., Močnik, G., and Herrmann, H.:  
749 Contributions of nitrated aromatic compounds to the light absorption of water-soluble and particulate brown  
750 carbon in different atmospheric environments in Germany and China, *Atmospheric Chemistry and Physics*, 17,  
751 1653-1672, 10.5194/acp-17-1653-2017, 2017.

752 Tuccella, P., Curci, G., Pitari, G., Lee, S., and Jo, D. S.: Direct radiative effect of absorbing aerosols: sensitivity to  
753 mixing state, brown carbon and soil dust refractive index and shape, *Journal of Geophysical Research:  
754 Atmospheres*, 125, e2019JD030967, 10.1029/2019JD030967, 2020.

755 Turpin, B. J., and Lim, H.-J.: Species contributions to PM<sub>2.5</sub> mass concentrations: Revisiting common assumptions  
756 for estimating organic mass, *Aerosol Science and Technology*, 35, 602-610, 10.1080/02786820119445, 2001.

757 Wang, X., Heald, C. L., Ridley, D. A., Schwarz, J. P., Spackman, J. R., Perring, A. E., Coe, H., Liu, D., and Clarke,  
758 A. D.: Exploiting simultaneous observational constraints on mass and absorption to estimate the global direct  
759 radiative forcing of black carbon and brown carbon, *Atmospheric Chemistry and Physics*, 14, 10989-11010,  
760 10.5194/acp-14-10989-2014, 2014.

761 Wathore, R., Mortimer, K., and Grieshop, A. P.: In-use emissions and estimated impacts of traditional, natural- and  
762 forced-draft cookstoves in rural Malawi, *Environmental Science & Technology*, 51, 1929-1938,  
763 10.1021/acs.est.6b05557, 2017.

764 Watson, J. G., Chow, J. C., Chen, L. W. A., and Frank, N. H.: Methods to assess carbonaceous aerosol sampling  
765 artifacts for IMPROVE and other long-term networks, *Journal of the Air & Waste Management Association*, 59,  
766 898-911, 10.3155/1047-3289.59.8.898, 2009.

767 Xie, M., Hannigan, M. P., Dutton, S. J., Milford, J. B., Hemann, J. G., Miller, S. L., Schauer, J. J., Peel, J. L., and  
768 Vedal, S.: Positive matrix factorization of PM<sub>2.5</sub>: Comparison and implications of using different speciation data  
769 sets, *Environmental Science & Technology*, 46, 11962-11970, 10.1021/es302358g, 2012.

770 Xie, M., Hannigan, M. P., and Barsanti, K. C.: Gas/particle partitioning of n-alkanes, PAHs and oxygenated PAHs in  
771 urban Denver, *Atmospheric Environment*, 95, 355-362, <http://dx.doi.org/10.1016/j.atmosenv.2014.06.056>, 2014.

772 Xie, M., Chen, X., Hays, M. D., Lewandowski, M., Offenberg, J., Kleindienst, T. E., and Holder, A. L.: Light  
773 absorption of secondary organic aerosol: Composition and contribution of nitroaromatic compounds,  
774 *Environmental Science & Technology*, 51, 11607-11616, 10.1021/acs.est.7b03263, 2017a.

775 Xie, M., Hays, M. D., and Holder, A. L.: Light-absorbing organic carbon from prescribed and laboratory biomass  
776 burning and gasoline vehicle emissions, *Scientific Reports*, 7, 7318, 10.1038/s41598-017-06981-8, 2017b.

777 Xie, M., Shen, G., Holder, A. L., Hays, M. D., and Jetter, J. J.: Light absorption of organic carbon emitted from  
778 burning wood, charcoal, and kerosene in household cookstoves, *Environmental Pollution*, 240, 60-67,  
779 <https://doi.org/10.1016/j.envpol.2018.04.085>, 2018.

780 Xie, M., Chen, X., Hays, M. D., and Holder, A. L.: Composition and light absorption of N-containing aromatic  
781 compounds in organic aerosols from laboratory biomass burning, *Atmospheric Chemistry and Physics*, 19, 2899-  
782 2915, 10.5194/acp-19-2899-2019, 2019.

783 Xie, M., Piedrahita, R., Dutton, S. J., Milford, J. B., Hemann, J. G., Peel, J. L., Miller, S. L., Kim, S.-Y., Vedal, S.,  
784 Sheppard, L., and Hannigan, M. P.: Positive matrix factorization of a 32-month series of daily PM<sub>2.5</sub> speciation  
785 data with incorporation of temperature stratification, *Atmospheric Environment*, 65, 11-20,  
786 <http://dx.doi.org/10.1016/j.atmosenv.2012.09.034>, 2013.

787 Yang, M., Howell, S. G., Zhuang, J., and Huebert, B. J.: Attribution of aerosol light absorption to black carbon,  
788 brown carbon, and dust in China – interpretations of atmospheric measurements during EAST-AIRE,  
789 *Atmospheric Chemistry and Physics*, 9, 2035-2050, 10.5194/acp-9-2035-2009, 2009.

790 Zhang, X., Lin, Y.-H., Surratt, J. D., and Weber, R. J.: Sources, composition and absorption Ångström exponent of  
791 light-absorbing organic components in aerosol extracts from the Los Angeles basin, *Environmental Science &*  
792 *Technology*, 47, 3685-3693, 10.1021/es305047b, 2013.



Table 1. Average concentrations of total NACs and tNAC<sub>OC</sub>% in Q<sub>f</sub> and Q<sub>b</sub> samples by fuel type and WBT phase.

Fuel & Test phase	Red Oak		Charcoal	
	CS	HS <sup>a</sup>	CS	HS
<b>Front filter (Q<sub>f</sub>)</b>				
Sample number	18	17 <sup>b</sup>	15	15
total NAC (µg m <sup>-3</sup> )	3.43 ± 1.37	3.91 ± 2.06	0.51 ± 0.43	1.00 ± 0.48
tNAC <sub>OC</sub> %	1.01 ± 1.06	0.98 ± 1.09	0.40 ± 0.25	0.31 ± 0.21
OC (µg m <sup>-3</sup> ) <sup>c</sup>	624 ± 410	908 ± 885	115 ± 72.0	447 ± 271
EC/OC <sup>c</sup>	1.74 ± 1.42	1.96 ± 1.74	6.12 ± 2.76	0.029 ± 0.012
<b>Backup filter (Q<sub>b</sub>)</b>				
Sample number	18	17 <sup>b</sup>	14 <sup>b</sup>	15
total NAC (µg m <sup>-3</sup> )	1.67 ± 0.76	1.79 ± 0.77	0.37 ± 0.31	1.30 ± 0.70
tNAC <sub>OC</sub> %	3.31 ± 3.46	2.77 ± 2.66	1.10 ± 0.89	1.08 ± 0.51
OC (µg m <sup>-3</sup> ) <sup>c</sup>	78.4 ± 43.2	100 ± 58.4	41.9 ± 23.3	138 ± 70.8
<b>Q<sub>b</sub>/Q<sub>f</sub> ratio (%)</b>				
total NACs	50.8 ± 13.4	53.4 ± 26.2	84.1 ± 38.0	140 ± 52.9
OC <sup>c</sup>	14.8 ± 3.87	15.3 ± 6.37	35.4 ± 12.2	38.8 ± 18.9

<sup>a</sup> Including three SIM phase samples from the 3-stone fire; <sup>b</sup> one filter sample was missed for analysis; <sup>c</sup> data were obtained from Xie et al. (2018).

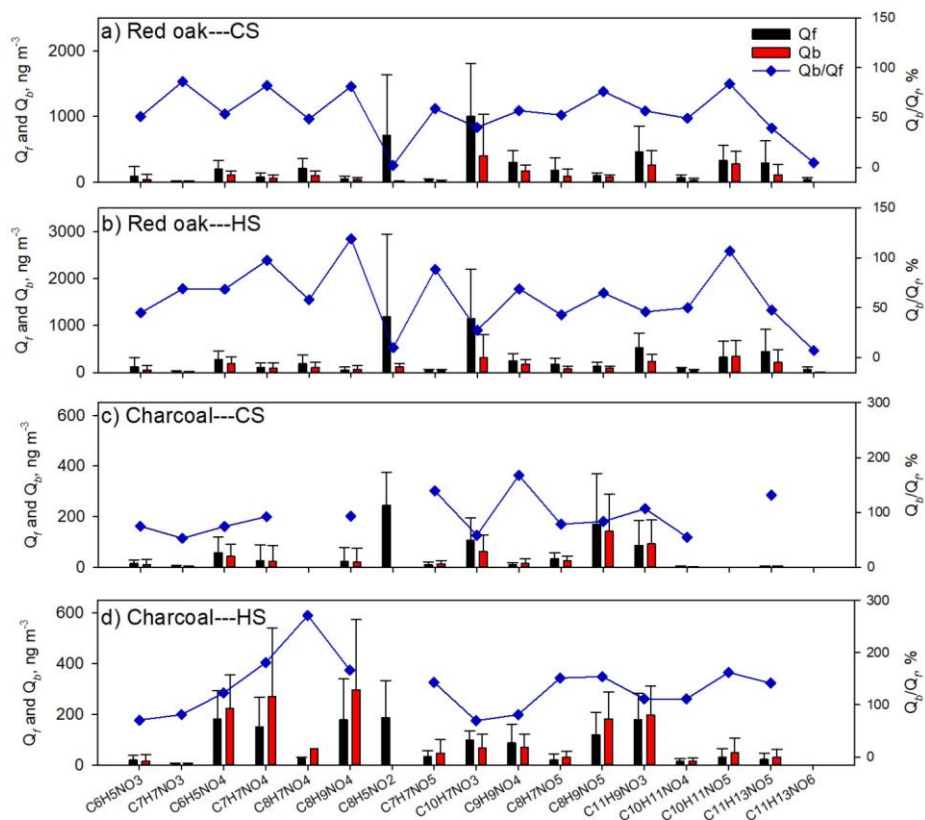


Figure 1. Average concentrations of individual NACs in  $Q_f$  and  $Q_b$  samples for (a) red oak burning under the CS phase, (b) red oak burning under the HS phase, (c) charcoal burning under the CS phase, and (d) charcoal burning under the HS phase. The blue scatters in each plot are mass ratios of individual NACs in  $Q_b$  to  $Q_f$  samples  $\times 100\%$ .

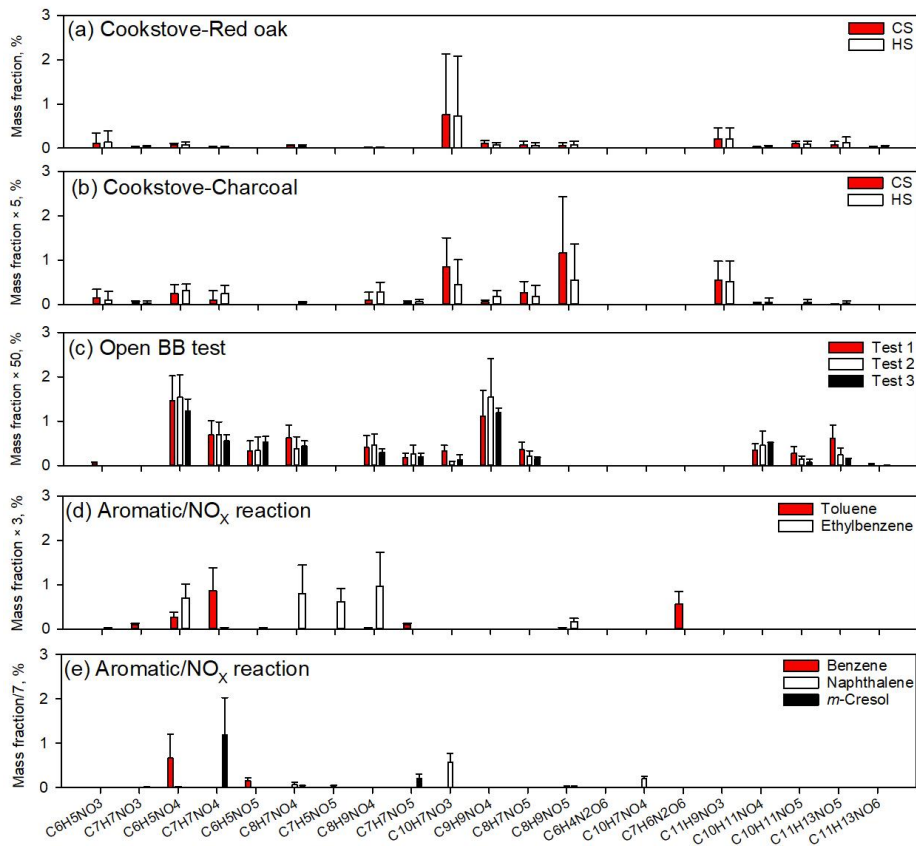


Figure 2. Average mass ratios (%) of individual NACs to organic matter from (a) red oak burning in cookstoves, (b) charcoal burning in cookstoves, (c) open BB experiments (Xie et al., 2019), photochemical reactions of (d) toluene and ethylbenzene, and (e) benzene, naphthalene, and m-cresol with  $\text{NO}_x$  (Xie et al., 2017a).

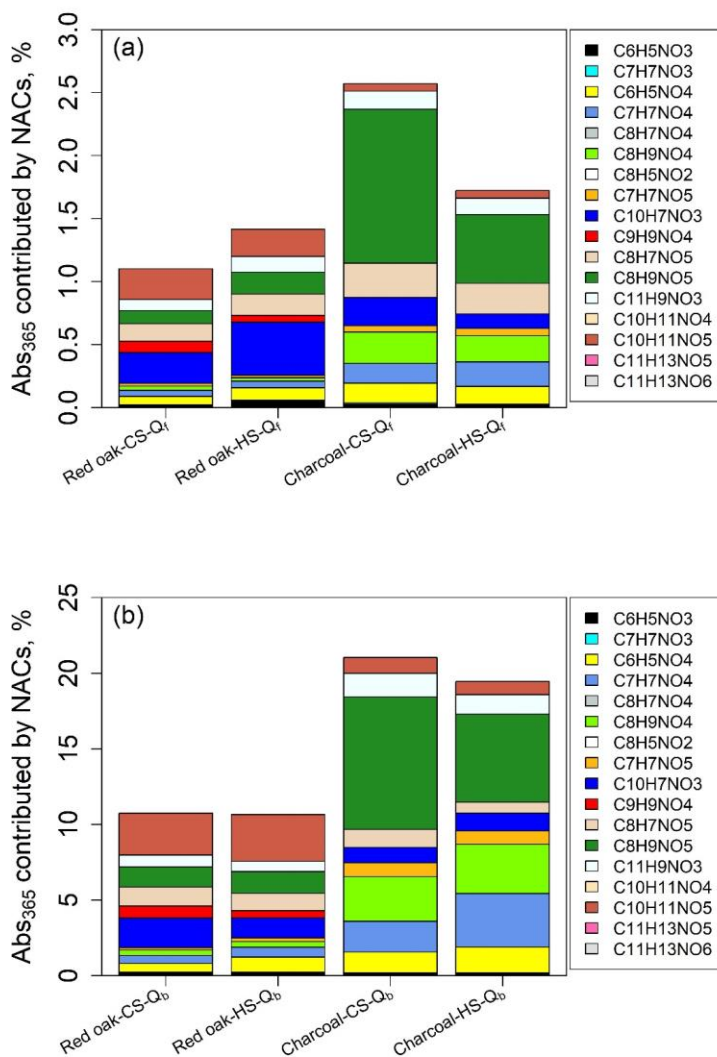


Figure 3. Average contributions (%) of individual NACs to bulk extracts Abs<sub>365</sub> of (a) Q<sub>f</sub>, and (b) Q<sub>b</sub> samples from burning red oak and charcoal in cookstoves under CS and HS phases.